

International
Progress Report

IPR-00-22

Äspö Hard Rock Laboratory

Deconvolution of breakthrough curves from TRUE-1 tracer tests (STT-2) with sorbing tracers

Äspö Task Force, Task 4F

Mark Elert, Håkan Svensson

Kemakta Konsult AB

June 2000

Svensk Kärnbränslehantering AB

Swedish Nuclear Fuel
and Waste Management Co
Box 5864
SE-102 40 Stockholm Sweden
Tel 08-459 84 00
+46 8 459 84 00
Fax 08-661 57 19
+46 8 661 57 19



**Äspö Hard Rock
Laboratory**

Report no.	No.
IPR-00-22	
Author	Date
Mark Elert	
Håkan Svensson	2000-06-01
Checked by	Date
Peter Wikberg	2000-10-20
Approved	Date
Olle Olsson	2000-11-01

Äspö Hard Rock Laboratory

Deconvolution of breakthrough curves from TRUE-1 tracer tests (STT-2) with sorbing tracers

Äspö Task Force, Task 4F

Mark Elert, Håkan Svensson

Kemakta Konsult AB

June 2000

Keywords: Äspö, transport of solutes, sorbing tracer tests, deconvolution

This report concerns a study which was conducted for SKB. The conclusions and viewpoints presented in the report are those of the author(s) and do not necessarily coincide with those of the client.

Abstract

The report presents deconvolution of the experimental results from the sorbing tracer experiment STT-2 performed within the Tracer Retention Understanding Experiments (TRUE) programme at the Äspö Hard Rock Laboratory. Deconvolution is a mathematical treatment of the tracer test data where the experimental tracer injection curves and breakthrough curves are used to evaluate what the breakthrough curve would have looked like if the injection was performed as a pulse with unit mass and zero duration (Dirac function). A short description of the experiments and a discussion of different methods for deconvolution are given. Deconvolution appears to be a useful approach to evaluate tracer experiments in order to identify features in the breakthrough curves caused by transport processes. In particular the deconvoluted curves can be used for comparison with unit response functions obtained from model predictions. The method presently used for deconvolution has successfully deconvoluted most of the tracers used in the STT-2 test.

Executive Summary

The Tracer Retention Understanding Experiments (TRUE) programme includes tracer tests at different experimental scales at the Äspö Hard Rock Laboratory. Within the first stage, TRUE-1, a series of tracer experiments has been performed between packed off boreholes in a single feature using both non-sorbing and sorbing tracers. In support of the TRUE-1 tracer tests the Äspö Task Force on Modelling of Groundwater Flow and Transport of Solutes has performed predictive modelling of the TRUE-1 tracer tests. Tasks 4C and 4D comprised predictive modelling of the radially converging tracer tests (RC-1) and dipole tracer tests (DP-1 – DP-4) performed within the TRUE-1 tests using non-sorbing tracers. In Tasks 4E and 4F of the Äspö Modelling Task Force predictive modelling of the sorbing tracer tests (STT-1, STT-1b and STT-2) is performed.

In order to facilitate the evaluation of the transport properties from the tracer tests it is important to have a well-defined injection source term that is short in comparison with the tracer travel time. In practice this may be difficult to achieve, which was the case for the non-sorbing tracer tests where a decaying pulse injection was used. The injection methods have been improved for the tests with sorbing tracers by introducing a finite pulse injection. In the STT-tests the tracer solution was replaced by unlabeled water after a few hours, which resulted in a finite pulse with only a slight decay due to dilution. In the STT-1b and STT-2 test replacement with unlabeled water was performed twice.

To evaluate the breakthrough curves excluding the effects caused by the injection procedure a mathematical treatment of the tracer test data can be done. This treatment, called deconvolution, uses the experimental tracer injection curves and breakthrough curves to evaluate what the breakthrough curve would have looked like if the injection was performed as a pulse with unit mass and zero duration (Dirac function). Ideally, all features of the resulting curve - the unit response function - are caused by processes occurring during the transport. In reality experimental errors may cause oscillations or mathematical artefacts in the unit response function. Therefore, mathematical manipulation of the experimental curves in the form of smoothing or curve fitting may be needed.

In this report a deconvolution of the experimental results from the sorbing tracer experiment STT-2 is presented. A short description of the experiments and a discussion of different methods for deconvolution are given. It is concluded that deconvolution is a useful approach to evaluate tracer experiments in order to identify features in the breakthrough curves caused by transport processes. In particular they can be used for comparison with unit response functions obtained from model predictions. The method presently used for deconvolution has successfully deconvoluted most of the tracers used in the STT-1 and STT-1b tests. However, there is a need for further improvement of the method in order to handle curves with large experimental errors.

Contents

	Page	
1	Introduction	6
1.1	Background	6
1.2	Äspö Modelling Task Force	6
1.3	Deconvolution	7
2	Tracer tests with sorbing tracers (STT-2)	10
2.1	Experimental setup	11
2.1.1	Equipment	11
2.1.2	Tracers used	11
2.1.3	Injection and sampling	12
2.2	Modelling Task 4F	12
3	Deconvolution approach	13
3.1	Introduction	13
3.2	Deconvolution techniques	14
3.3	Mathematical treatment of experimental data	16
3.4	Convolution of the unit response function	16
3.5	Calculation algorithm	17
4	Results of deconvolution	19
4.1	Experimental results	19
4.1.1	Tracer test SST-2	19
4.2	Deconvolution of STT-2 test	20
4.3	Comparison of results	38
5	Discussion and conclusions	39
5.1	Deconvolution approach	39
5.2	Deconvolution methods	39
5.3	Conclusions	40
	References	34

List of Figures

Figure 1-1	Tracer injection and breakthrough in RC-1.	7
Figure 1-2	Tracer injection and breakthrough in DP-1.	7
Figure 1-3	Tracer injection and breakthrough in STT-1b.	8
Figure 1-4	Tracer injection and breakthrough of uranine in STT 2.	8
Figure 2-1	Test geometry and borehole intersection pattern with Feature A.	10
Figure 3-1	Principle of convolution.	13
Figure 3-2	Principle of deconvolution.	14
Figure 4-1	Injection concentration versus time for STT-2.	19
Figure 4-2	Breakthrough concentrations for STT-2.	20
Figure 4-3	Unit response function for Uranine in STT-2.	21
Figure 4-4	Convolved unit response function for Uranine in STT-2 compared with measured data.	22
Figure 4-5	Interpolated input curve for Uranine in STT-2.	22
Figure 4-6	Unit response function for HTO in STT-2.	23
Figure 4-7	Convolved unit response function for HTO in STT-2 compared with measured data.	23
Figure 4-8	Original and filtered output data for HTO in STT-2.	24
Figure 4-9	Unit response function for Br-82 in STT-2.	24
Figure 4-10	Convolved unit response function for Br-82 in STT-2 compared with measured data.	25
Figure 4-11	Original and filtered output data for Br-82 in STT-2.	25
Figure 4-12	Unit response function for Na-22 in STT-2.	26
Figure 4-13	Convolved unit response function for Na-22 in STT-2 compared with measured data.	26
Figure 4-14	Original and filtered output data for Na-22 in STT-2.	27
Figure 4-15	Unit response function for Sr-85 in STT-2.	27
Figure 4-16	Convolved unit response function for Sr-85 in STT-2 compared with measured data.	28
Figure 4-17	Original and filtered output data for Sr-85 in STT-2.	28
Figure 4-18	Unit response function for Ca-47 in STT-2.	29
Figure 4-19	Convolved unit response function for Ca-47 in STT-2 compared with measured data.	29
Figure 4-20	Original and filtered output data for Ca-47 in STT-2.	30

Figure 4-21	Unit response function for Ba-131 in STT-2.	30
Figure 4-22	Convolved unit response function for Ba-131 in STT-2 compared with measured data.	31
Figure 4-23	Original and filtered output data for Ba-131 in STT-2.	31
Figure 4-24	Unit response function for Ba-133 in STT-2.	32
Figure 4-25	Convolved unit response function for Ba-133 in STT-2 compared with measured data.	32
Figure 4-26	Original and filtered output data for Ba-133 in STT-2.	33
Figure 4-27	Unit response function for Rb-86 in STT-2.	33
Figure 4-28	Original and filtered output data for Rb-86 in STT-2.	34
Figure 4-29	Unit response function for Cs-134 in STT-2.	34
Figure 4-30	Original and filtered output data for Cs-134 in STT-2.	35
Figure 4-31	Effect of different filter length on the deconvolution of Rb-86 breakthrough in STT-2. Left hand column gives the unit response functions and the right hand column the filtered breakthrough curves. a) 3-step normal filter, b) 7-step normal filter, c) 11-step normal filter, d) 11-step uniform filter.	36
Figure 4-32	Original and fitted breakthrough data for Cs-134 in STT-2.	37
Figure 4-33	Unit response function for Cs-134 in STT-2, the output data in the deconvolution calculation is calculated from the function fitted on experimental breakthrough curve.	38
Figure 4-34	Unit response functions for tracers in STT-2.	38

List of Tables

Table 2-1	Tracers used in STT-2.	11
Table 4-1	Time steps, filtering and matrix inversion method used for deconvolution of the STT-2 tracer test results.	21

1 Introduction

1.1 Background

The Äspö Hard Rock Laboratory (HRL) is an underground research facility situated on the east coast of Sweden operated by the Swedish Nuclear Fuel and Waste Management Company (SKB). The Äspö HRL provides opportunities to perform studies of behaviour and properties of the natural geological barriers, investigate interactions between engineered barriers and the host rock, and perform development and demonstration of technology for deep repository systems.

Within the Äspö Hard Rock Laboratory project a programme called Tracer Retention Understanding Experiments (TRUE) has been defined for tracer tests at different experimental scales. The overall objective of the TRUE programme is to increase the understanding of the processes which govern retention of radionuclides transported in crystalline rock, and to increase the credibility in the computer models for radionuclide transport which will be used in the licensing of a repository. Within the first stage, TRUE-1, a series of tracer experiments have been performed in a single feature using both non-sorbing and sorbing tracers.

1.2 Äspö Modelling Task Force

The Äspö Task Force on Modelling of Groundwater Flow and Transport of Solutes was initiated by SKB in 1992 as a forum for the organisations supporting the Äspö HRL Project. The purpose of the Task Force is to interact in the area of conceptual and numerical modelling of groundwater flow and solute transport in fractured rock. In particular, the Task Force proposes, reviews, evaluates and contributes to such work in the HRL Project.

Task 4 of the Äspö Modelling Task Force consists of modelling exercises in support of the TRUE-1 tracer tests. Tasks 4C and 4D comprised predictive modelling of the radially converging tracer tests (RC-1) and dipole tracer tests (DP-1 – DP-4) performed within the TRUE-1 tests using non-sorbing tracers. The tests were performed between packed off boreholes penetrating a water-conducting geological feature with a simple structure (Feature A). These tests have been followed by tests with sorbing radioactive tracers (STT-1, STT-1b and STT-2) in the same feature. In Tasks 4E and 4F of the Äspö Modelling Task Force predictive modelling of the sorbing tracer tests is performed.

1.3 Deconvolution

In order to facilitate the evaluation of the transport properties from the tracer tests it is important to have a well-defined injection source term that is short in comparison with the tracer travel time. In practice this may be difficult to achieve. In the radially converging test tracers a decaying pulse injection was used. Tracers were injected in the borehole sections and initially circulated in order to achieve a rapid homogenisation. Thereafter, the tracer concentration in the injection section decreased slowly due to the induced flow obtained by the pumping. Due to the low flow rates and the relatively large volumes of the injection sections, the decay of the injection pulse was slow. The time until the concentration reached half its original value was of the same magnitude as the median breakthrough time of the tracers (Figure 1-1).

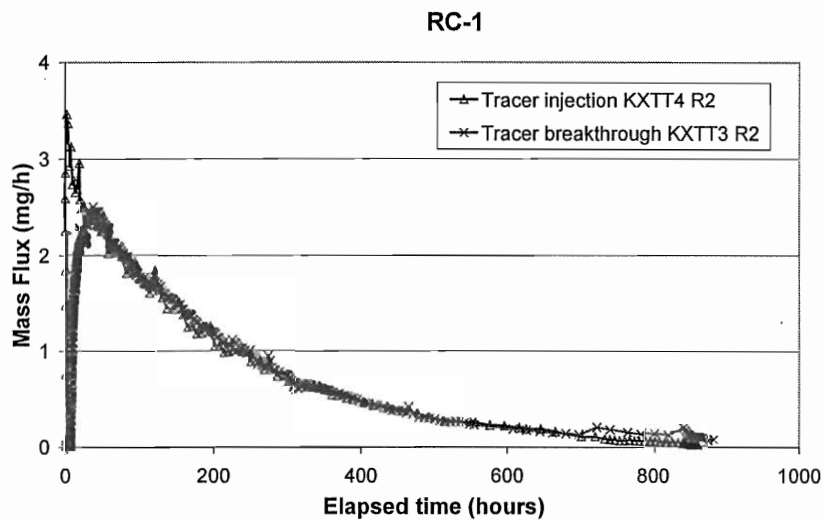


Figure 1-1 Tracer injection and breakthrough in RC-1.

The same methodology was also used in the dipole tests (DP). However, the decay of the pulse was much faster due to the flow induced by the injection of unlabeled water in the injection sections (Figure 1-2).

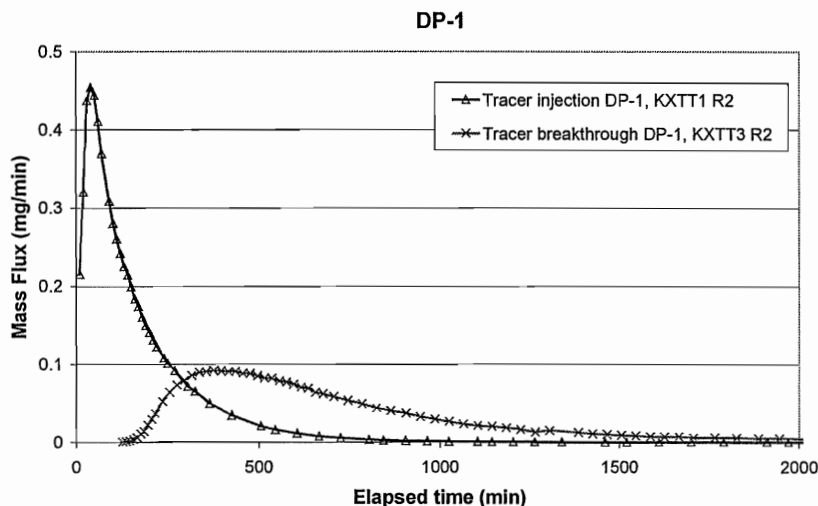


Figure 1-2 Tracer injection and breakthrough in DP-1.

In STT-1 and STT 1-b experiments the injection method were improved for the tests with sorbing tracers by introducing a finite pulse injection. In these tests the tracer solution was replaced by unlabeled water after a few hours, after which the tracer concentration in the injection section decreased rapidly by a factor of 30. This resulted in a finite pulse with only a slight decay due to dilution. After the replacement of the injection fluid the tracer concentration increased slightly again (Figure 1-3).

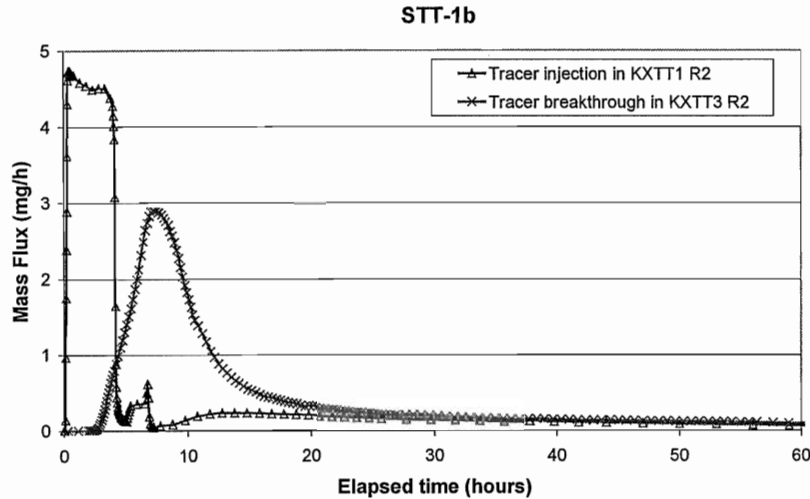


Figure 1-3 Tracer injection and breakthrough in STT-1b.

The same methodology was used in the STT-2 test but with a decreased flow rate. To get an even more efficient ending of tracer pulse the exchange procedure with unlabeled water was repeated twice during STT-2 (Figure 1-4).

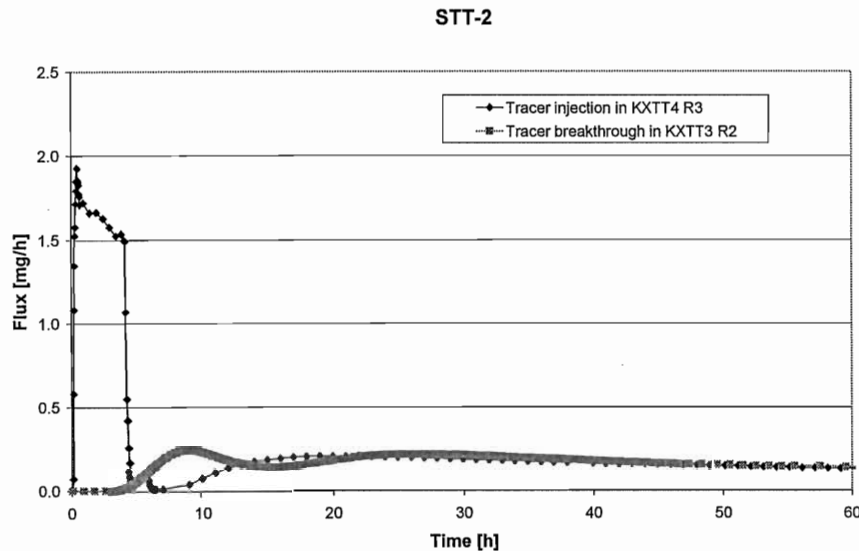


Figure 1-4 Tracer injection and breakthrough of uranine in STT 2.

To evaluate the breakthrough curves excluding the effects caused by the injection procedure a mathematical treatment of the tracer test data can be done. This treatment, called deconvolution, uses the experimental tracer injection curves and breakthrough curves to evaluate what the breakthrough curve would have looked like if

the injection was performed as a pulse with unit mass and zero duration (Dirac function). Ideally, all features of the resulting curve - the unit response function - are caused by processes occurring during the transport. In reality experimental errors may cause oscillations or mathematical artefacts in the unit response function. Therefore, mathematical manipulation of the experimental curves in the form of smoothing or curve fitting may be needed.

In this report deconvolution of the experimental results from the sorbing tracer experiments STT-2 is presented. The report also gives a short description of the experiments and discusses different methods for deconvolution. Previously, deconvolution has been performed for the tracer tests STT-1 and STT-1b (Elert and Svensson, 1999).

2 Tracer tests with sorbing tracers (STT-2)

The tracer test STT-2 was performed between different borehole sections penetrating Feature A. A detailed experimental description of STT-2 is given in Andersson et al. (1999). The main objective for the tracer tests with sorbing tracers was to test equipment and procedures for tests with radioactive sorbing tracers to be performed in later stages of the TRUE Project. Secondly, to increase the understanding of transport and retention of sorbing species in crystalline rock. The purpose of STT-2 was to obtain in-situ sorption data in feature A and to study the influence of a decreased flow rate on the transport of radionuclides compared to STT-1 and STT-1b.

STT-2 was performed in Feature A in a radially converging flow geometry between borehole sections KXTT4 R3 → KXTT3 R2 that is the same flow path as STT-1, see Figure 2-1. The pumping rate was 0.201 l/min. In total twelve tracers, three conservative (Uranine, tritiated water and ^{82}Br) and nine weakly to moderately radioactive sorbing tracers (^{22}Na , ^{42}K , ^{47}Ca , ^{85}Sr , $^{99\text{m}}\text{Tc}$, ^{131}Ba , ^{133}Ba , ^{86}Rb and ^{137}Cs) were mixed and injected as a finite pulse with a duration of four hours.

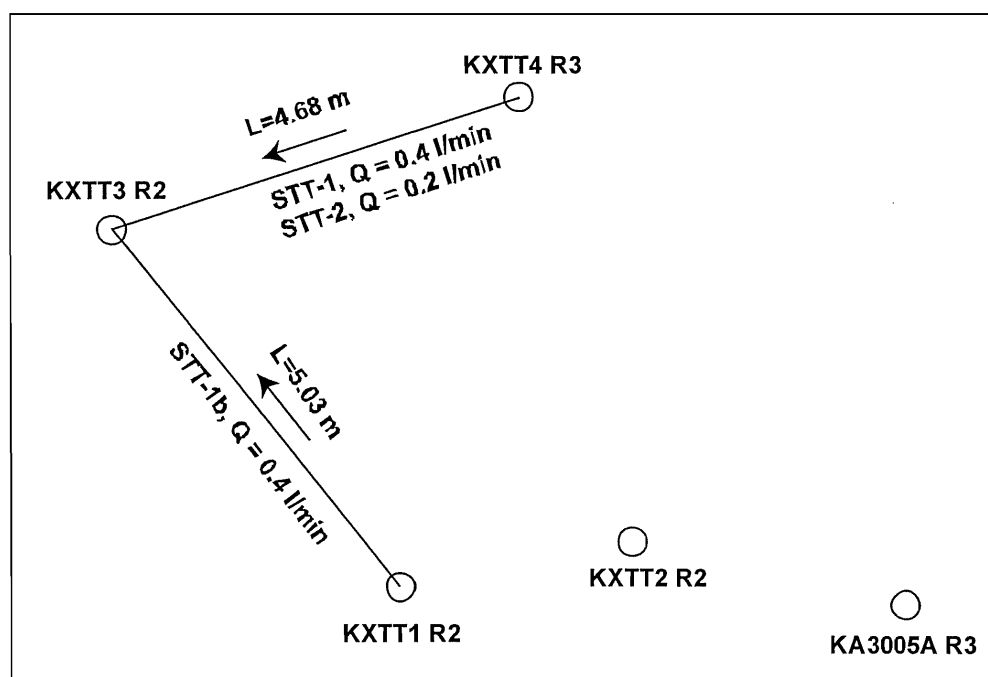


Figure 2-1 Test geometry and borehole intersection pattern with Feature A.

Tracer breakthrough in the pumping section was monitored for all tracers injected, except $^{99\text{m}}\text{Tc}$ and ^{42}K . The radioactive tracers were recovered in-line with a HpGe detector. The breakthrough curves show, for the conservative tracers, one narrow peak and a secondary almost equally high but wider peak. For the weakly sorbing tracers, the first peak is lower and not that distinct and for the moderately sorbing tracers it is not seen at all.

2.1 Experimental setup

2.1.1 Equipment

Each borehole in the TRUE-1 array is instrumented with inflatable packers such that 4-5 borehole sections are isolated. The borehole sections in Feature A were also equipped with volume reducers (dummies). The equipment was tested for sorption of the tracers used in STT-2 and no significant sorption could be detected. The borehole fluid is circulated in the injection borehole in order to obtain a homogeneous tracer concentration inside the borehole and to be able sample the tracer concentration outside the borehole. Circulation is controlled by a pump with variable speed and measured by a flow meter.

2.1.2 Tracers used

During STT-2, a mixture of in total twelve different tracers, both conservative and sorbing, was injected. The sorbing tracers used were nine radioactive, gamma-emitting, isotopes of mono- and divalent cations, see Table 2-1. These tracers needed to be injected in such low concentrations that the chemical conditions were kept unchanged in Feature A. Another restriction was the maximum permitted dose. The conservative tracers were Uranine (Sodium Fluorescein), tritiated water (HTO) and the radioactive gamma-emitting tracer ^{82}Br .

Table 2-1 Tracers used in STT-2.

Name	Isotope	Half-life
Uranine	-	-
HTO	^3H	12.3 a
Bromine	^{82}Br	35.3 h
Sodium	^{22}Na	2.6 a
Calcium	^{47}Ca	4.5 d
Strontium	^{85}Sr	65 d
Potassium	^{42}K	12.4 h
Technetium	$^{99\text{m}}\text{Tc}$	6.0 h
Barium	^{131}Ba	11.5 a
Barium	^{133}Ba	10.5 a
Rubidium	^{86}Rb	19 d
Caesium	^{134}Cs	2.1 a

2.1.3 Injection and sampling

The tracer solution (3.5 litres) containing all twelve tracers was mixed with synthetic groundwater and mixed into a tracer stock solution with the non-sorbing tracers HTO and Uranine. The injection of tracer was made in the circulation loop as a finite pulse injection with a length of four hours. After four hours of injection the tracer solution was exchanged with unlabelled water. The exchange procedure lasted for 50 minutes. A second exchange was made one hour after the end of the first one to achieve an even more efficient exchange. The latter exchange lasted for 40 minutes.

The tracer concentration in the injection loop is measured both in situ using a HPGe-detector and by sampling and subsequent analysis in the laboratory. The sampling is made by continuously extracting a small volume of water from the system through a flow controller (constant leak) to a fractional sampler. The decrease in injection concentration was measured by sampling for Uranine and HTO with samples taken every 2nd minute during the initial 40 minutes of injection, and then every 30 minutes up to four hours. The sampling frequency was then increased again to one sample every 4th minute during the exchange procedure. After that samples were taken once every hour. After some months the sampling frequency was gradually decreased to one sample/10 hours. The radionuclides were measured with the on-line detector with a somewhat higher frequency than the discrete sampling during the first seven hours. After that activity measurements were made over a period of one hour gradually decreasing to 24 hour periods at later stages of the sampling (~500 hours).

The sampling system in the pumping borehole is based on the same principle as the injection system, namely a circulating system with a circulation pump and a flow meter. The sampling was made with two independent systems, a "constant leak" system producing 8 ml samples integrated over a period between 5 and 100 minutes, and a 24-valve sampling unit producing 1 litre samples discrete in time. Both systems took samples every 10th minute during the first 13 hours, thereafter the decreasing sampling frequency gradually decreased down to one sample/96 hours at the end of the test period.

2.2 Modelling Task 4F

The Äspö Task Force modelling Task 4F was defined with the overall objectives of developing the understanding of radionuclide migration and retention in fractured rock and evaluating the usefulness and feasibility of different approaches to model radionuclide migration of sorbing species based on existing in situ and laboratory data from the TRUE-1 site.

The task includes predictive modelling of the sorbing tracer experiments STT-2. At the 13th Äspö Task Force Meeting in February 2000 nine modelling teams had submitted predictions of the tracer experiments.

3 Deconvolution approach

3.1 Introduction

Convolution and deconvolution techniques are used in signal processing and in other problems where the purpose is to analyse a linear system where the output function is given by an input function and a unit response function. For evaluation of tracer transport convolution can be used to obtain a breakthrough curve for a given injection curve when the unit response function is known, see Figure 3-1. Convolution is often used in mathematical modelling of solute transport. In this case a single unit response function for a system is calculated and then used to derive breakthrough curves for arbitrary input functions.

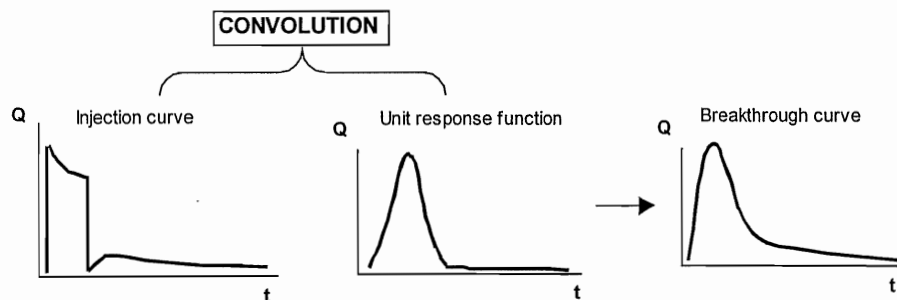


Figure 3-1 Principle of convolution.

The inverse of convolution is called deconvolution and can be used to find the unit response function from the injection curve and the breakthrough curve. The unit response function describes how the breakthrough curve would look like if the injection curve was a Dirac delta function, i.e. a pulse with unit mass and zero duration. In Figure 3-2 the deconvolution principle is described schematically.

The unit response function describes the characteristic features of the particular flow and transport problem determined by the transport mechanisms along the flowpaths. The unit response function is unaffected by the boundary conditions for the tracer, i.e. injection concentration as a function of time. Since any effects due to the shape of the injection curve is removed, the unit response function can be used as a diagnostic tool for identification of the relevant transport mechanisms, for example early time diagnostics, tailing and presence of multiple peaks. It can also be used for parameter estimation (porosity, dispersivity, etc.).

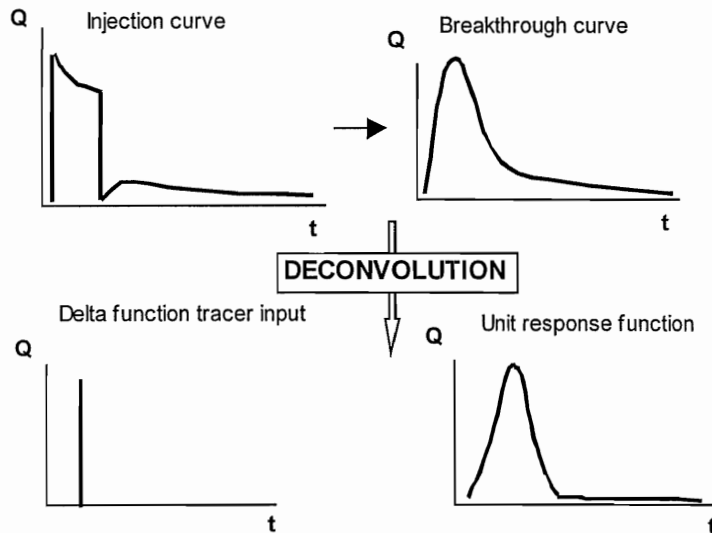


Figure 3-2 Principle of deconvolution.

The convolution and deconvolution is based on the superpositioning of solutions. It is therefore required that the transport processes are linear as regard to concentration and that they are invariant in time, i.e. processes such as non-linear sorption, etc cannot be treated.

3.2 Deconvolution techniques

Deconvolution is an ill-posed problem, small measurement errors in the injection and breakthrough curves may cause numerical problems (e.g. oscillations) and large errors in the calculated response functions. The physical constraints on the unit response function can be used to improve the solution. For example requirements on the stability of the obtained solution, the exclusion of negative values of the unit response function as they have no physical meaning.

A large range of techniques has been applied to problems in signal processing, astrophysics, geophysics and image processing. A basic method is the use of Fourier Transforms including various types of filtering techniques. However, Fourier transforms are not very suitable for deconvolution, e.g. due to spectral leakage (Ilvonen et al., 1994). Other techniques use the Kalman filter that gives an optimal estimate of a given process allowing for updates based on output measurements. However, the Kalman filter requires an accurate model of the system in order to achieve a good performance.

Several techniques have been used for deconvolution in connection with solute transport. In a method called regularisation a solution is found by minimising an objective function containing two terms, one that measures the fit of the solution and a second that measures other properties of the solution, e.g. smoothness (cf. Skaggs et al., 1998). Deconvolution of tracer test data from Finnsjön has been made using the Extreme Value Estimation Method (EVE) (Ilvonen et al., 1994) and the Toeplitz method (Tsang et al., 1991). The EVE method solves a linear set of equations where all

unknowns are required to be non-negative. Estimates are given of the upper and lower bands of the unknowns.

The deconvolution technique used in this report is based on the Toeplitz method (Tsang et al., 1991). The tracer injection mass flow rate m_j is given in discrete steps where j is the index for successive times. Also the tracer mass breakthrough M_i is discretized with i as the index for successive times. For each input element m_j at time t_j a unit response function a_{ij} is defined. The response function must fulfil some special properties. The response time i must be later than the input time j and the response function must be time invariant and therefore the response function a_{ij} is only a function of $t_i - t_j$ which means that $a_{ij} = a_{i-j}$. Then the output M_i can be given as the superposition for all the input elements (m_j) times the response function a_{i-j} :

$$M_i = \sum_j a_{ij} \cdot m_j$$

where

$$a_{ij} = a_{i+n, j+n} \quad (\text{time invariant})$$

$$a_{ij} = 0 \quad \text{for } i \leq j$$

The transfer coefficients a_{ij} defined as above is a Toeplitz matrix and because of its time invariance ($i-j$) it can be described as a vector a_s where $s = i-j$:

$$M_i = \sum_s m_{is} a_s$$

where

$$a_s = a_{ij} \quad s = i-j, i > j$$

$$m_{is} = m_j \quad j = i-s$$

$$m_{is} = 0 \quad i \leq s$$

The vector a_s , the response function to a unit pulse injection at the first time interval, and the m_{is} coefficients become in matrix form:

$$\mathbf{M} = \mathbf{m} \cdot \mathbf{a}$$

If this expression is inverted it gives the unit response function as:

$$\mathbf{a} = \mathbf{m}^{-1} \mathbf{M}$$

The different methods available in Matlab for matrix inversion have been tested:

- the "backslash" operator where $A \setminus B$ is the matrix division of A into B . For square systems (A is an N -by- N matrix and B is a column vector with N components), $X = A \setminus B$ is the solution to the equation $A * X = B$ computed by Gaussian elimination. For an under- or overdetermined system of equations $A * X = B$, the effective rank, K , of A is determined from the QR decomposition with pivoting. A solution X is computed which has at most K nonzero components per column.
- the function `nnls` (Non-negative least-squares) which calculates the vector X that minimizes $\text{NORM}(A * X - b)$ subject to X greater or equal to zero. Thus the non-physical solutions with negative unit response functions can be avoided.

- the function `pinv` which uses the Moore-Penrose pseudoinverse of a matrix non-square matrix.
- the function `cgs` which uses the Conjugate Gradients Squared method to iteratively solve the system of linear equations $A*x = b$ for x .

The Toeplitz method has proved to be considerably more stable than using the deconvolution routine (`deconv`) included in Matlab. With this routine it was not possible to obtain stable solutions for the unit response function with the original experimental data for any of the tracers.

3.3 Mathematical treatment of experimental data

Some of the breakthrough curves were highly irregular. The result of the deconvolution is very sensitive to the detailed shape of the breakthrough curve. Therefore, irregular breakthrough curves, e.g. spiky curves, were filtered. One alternative to filtering is curve fitting. However, curve fitting may either eliminate details that are present or introduce artificial details in the curves. Although filtering also is a manipulation of the results it was considered to create less potential problems than curve fitting. The Matlab function `filter(b,a,x)` was used as a moving average filter on the breakthrough concentration values. Below is an example of the algorithm presented for a case when averaging over a five hour window:

$$y(n) = \frac{1}{5}x(n-2) + \frac{1}{5}x(n-1) + \frac{1}{5}x(n) + \frac{1}{5}x(n+1) + \frac{1}{5}x(n+2)$$

x are the original breakthrough values
 y are the filtered breakthrough values
 n is the index of current sample

A problem with the algorithm described above is that the values covered in the interval of the moving average filter are equally weighted which results in negative effects on the shape of the filtered curve. This effect is especially noticeable at narrow peaks, which are flattened out as the interval of the moving average filter is increasing. To get a more optimised filtration an option of using normally distributed filter coefficients was introduced. With this option the central value ($x(n)$ in the example above) is given the highest weight. The weight of the filter coefficients is reduced towards the side of the filter. That is, the $x(n-1)$ and $x(n+1)$ values are given less weight and consequently the $x(n-2)$ and $x(n+2)$ values the least weight.

3.4 Convolution of the unit response function

To verify the accuracy of the unit response functions, calculated with the Toeplitz method, convolution has been done on the response functions and the corresponding injection curves. The original breakthrough curves from the tracer experiments are compared to the calculated breakthrough curves from the convolution. The convolution procedure used in this report is based on the Matlab function `conv(a,b)` which convolves vectors a and b :

$$c(k) = \sum_j a(j) \cdot b(k+1-j)$$

where

a is the unit response function of length m

b is the discrete injection mass flow rate of length n

c is the convoluted breakthrough curve of length $m+n-1$

3.5 Calculation algorithm

The program language MATLAB was chosen for solving the computing problems. MATLAB integrates computation and visualisation and it also offer predefined functions, as filtration functions, which facilitate the algorithm development. A flow chart summarising the algorithm for deconvolution is presented in Figure 3-3.

The result of the deconvolution is very sensitive to the detailed shape of both the injection and the breakthrough data. Especially, the experimental values of the first 0.5 hours of the injection concentration were very scattered. Therefore, a mean value is calculated for the first values of the injection concentration and represents the initial value of the injection curve. The breakthrough data is filtered with a moving average filter and there are options to adjust the filtering level dependent on the degree of the irregularity of the breakthrough data. Before the deconvolution, the injection and breakthrough data arrays are given an equidistant time step by interpolation of the experimental data.

There are four deconvolution method options which require symmetric matrixes and adjustment of injection and withdrawal data are made to set the data arrays to equal lengths. However, in most cases the injection data arrays are shorter than the breakthrough data arrays and therefore adding of zeroes is made to the injection arrays when necessary.

To facilitate the analysis the deconvolution program can loop through a series of consecutive calculations with different deconvolution methods and time steps. To verify the accuracy of the deconvoluted unit response function, convolution is made on the response function and the corresponding injection curve.

Finally plotting is made for the experimental data, unit response function and interpolated and filtered data curves.

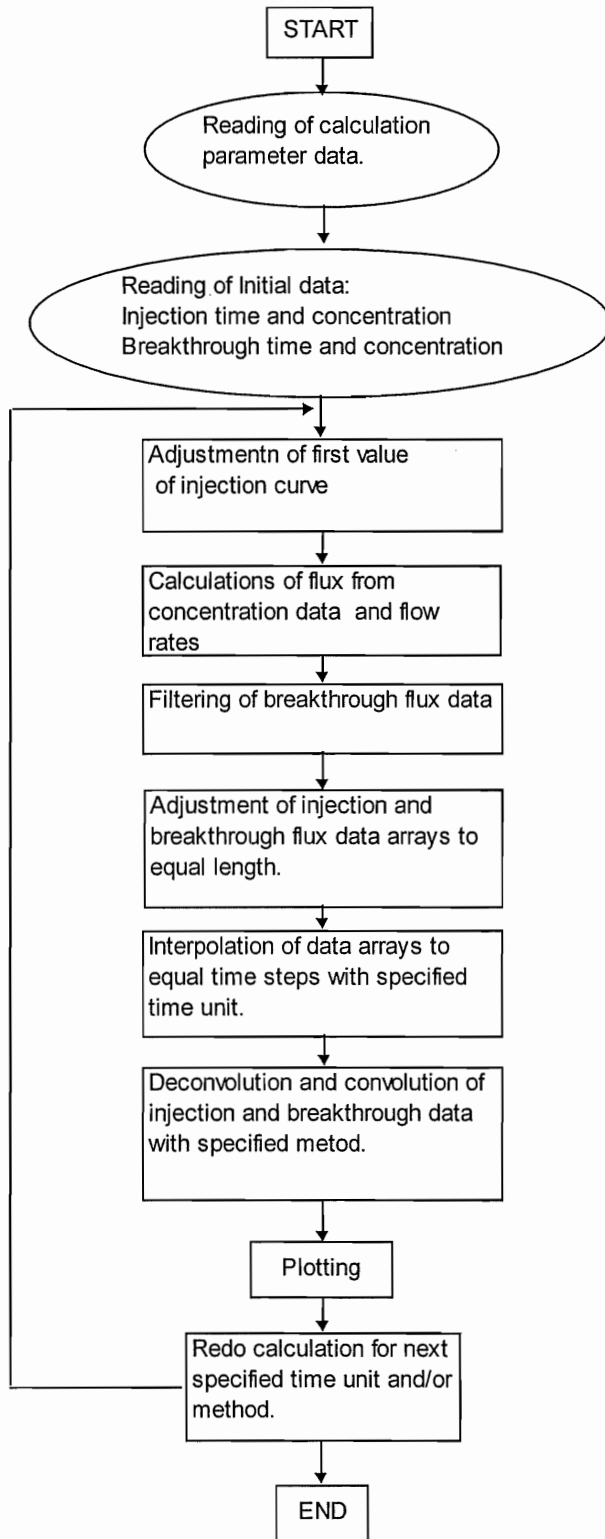


Figure 3-3 Flow chart for the algorithm for deconvolution calculations in MATLAB.

4 Results of deconvolution

4.1 Experimental results

4.1.1 Tracer test SST-2

The injection concentrations versus time for the different tracers in STT-2 are shown in logarithmic scale Figure 4-1. There is a sharp increase in concentration during the initial part of the injection, followed by a decline in concentration due to dilution by the flow through the borehole section. The decline is more pronounced for the sorbing radionuclides due to sorption on the borehole walls. After 4 hours the injection fluid was exchanged with unlabelled water which gives a rapid decrease in concentration by a factor 40. This is followed by an increase in concentration probably due to tracers remaining in a stagnant zone within the injection section. After about 7 hours a second exchange of water was made, which gives an additional decline in concentration. Finally, the concentration declines due to dilution.

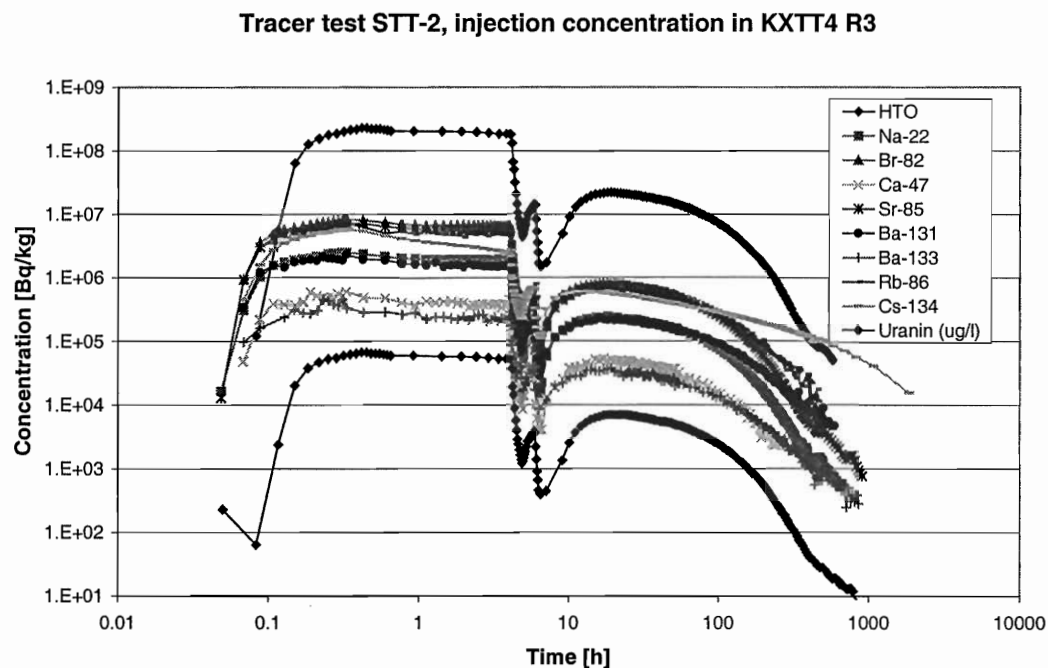


Figure 4-1 Injection concentration versus time for STT-2.

For all the tracers the experimental injection curves has approximately the same shape, the main difference is that the decrease in concentration occurs much faster for the more strongly sorbing species like Cs. This rapid decrease is the effect of sorption on the borehole walls in the injection section.

In STT-2 all of the injected tracers except Tc-99m and K-42 were recovered in the pumping section KXTT3 R2. Figure 4-2 shows the breakthrough concentration as a function of time in a logarithmic scale. For HTO, Br-82 and Uranine breakthrough occurs at a similar time and the curves also have a similar shape. For these tracers the breakthrough consists of two peaks. The breakthrough for Na-22, Ca-47 and Sr-85 occurs a little bit later but still with a clear indication of two peaks. For Rb-86, Ba-131, Ba-133 and Cs-134 the breakthrough occurs at a later time and the breakthrough curves have only one peak.

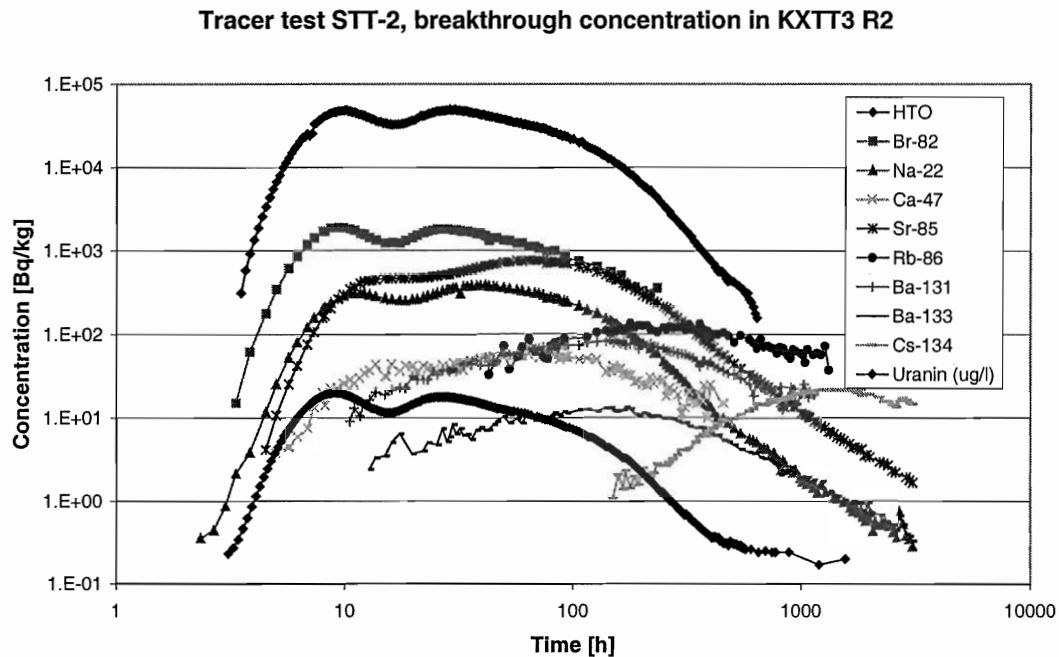


Figure 4-2 Breakthrough concentrations for STT-2.

4.2 Deconvolution of STT-2 test

Deconvolution of the experimental results from the STT-1 test has been performed on the tracers: Ba-131, Ba-133, Br-82, Ca-47, Cs-134, HTO, Na-22, Rb-86, Sr-85 and Uranine. For all the tracers the deconvolution could be performed on the experimental data without curve-fitting. However, different degrees of filtering were performed on the breakthrough curves. A series of tests were made varying the time step, the filter option and the matrix inversion method. It was found that a time step of 2 hours was optimal for most tracers. A shorter time step resulted in extensive oscillations in the breakthrough curve and longer time step concealed much of the details in the early arrival. An exception was Cs-134, for which a time step of 3 seconds was needed. A study of the effect of varying the filter length is presented in Section 4.3.

The time step, the filtering of data and the matrix inversion method used for the final deconvolution the different tracer breakthrough curves are summarised in Table 4-1.

Table 4-1 Time steps, filtering and matrix inversion method used for deconvolution of the STT-2 tracer test results.

Tracer	Start time (h)	Time step (h)	Filter type	Flevel	Inversion method
Uranine	0.4	2	no filtering	0	backslash
HTO	0.4	2	3-step normal	1	backslash
Br-82	0.2	2	3-step normal	1	backslash
Na-22	0.2	2	5-step normal	2	backslash
Sr-85	0.4	2	3-step normal	1	backslash
Ca-47	0.2	2	9-step normal	4	backslash
Ba-131	0.2	2	7-step normal	3	backslash
Ba-133	0.2	2	9-step normal	4	backslash
Rb-86	0.2	2	15-step uniform	4	backslash
Cs-134	0.2	3	5-step normal	2	backslash

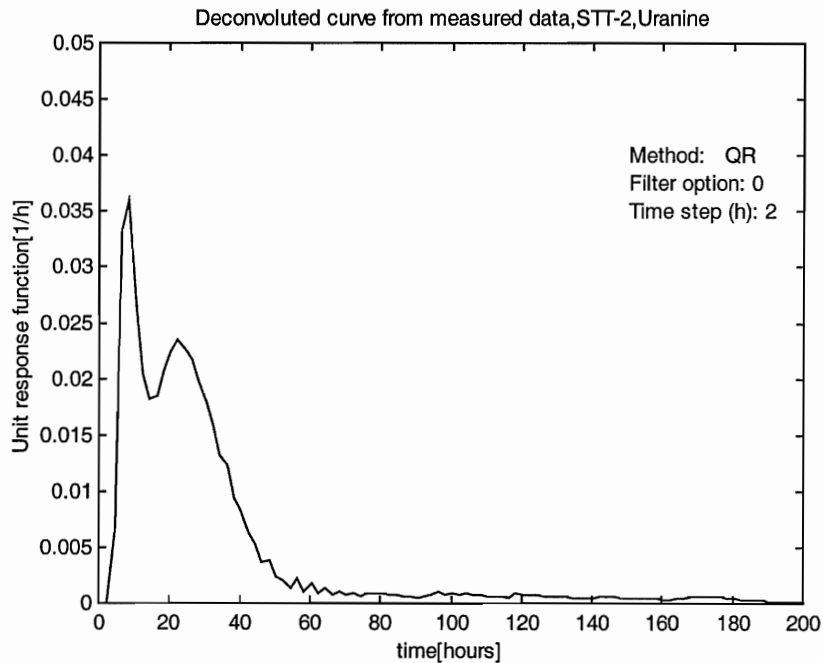


Figure 4-3 Unit response function for Uranine in STT-2.

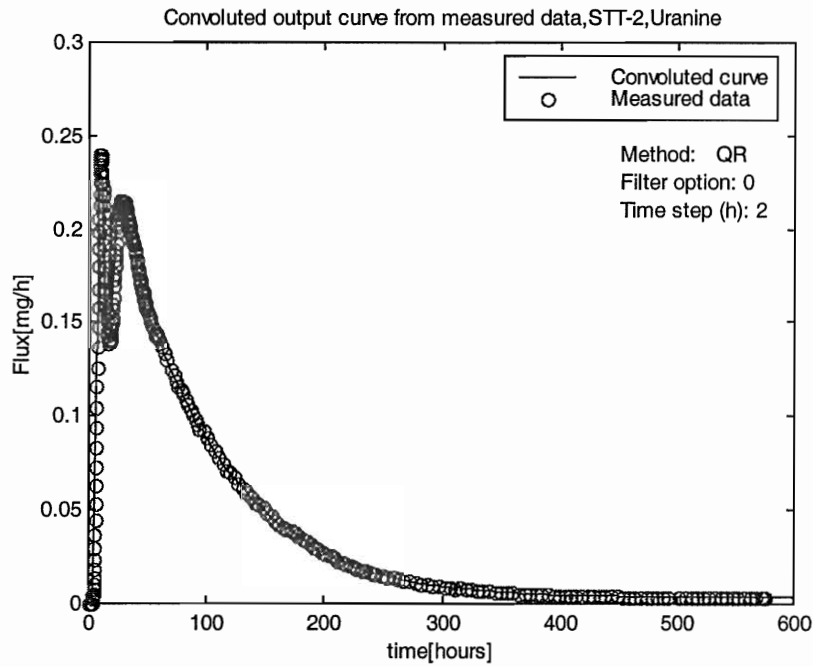


Figure 4-4 *Convoluted unit response function for Uranine in STT-2 compared with measured data.*

The deconvoluted curve for Uranine shows two distinct peaks and almost no tailing. The breakthrough curve was relatively smooth and therefore no filtering was necessary. A convolution of the unit response function with the injection curve gives results very similar to the measurements, which indicates a successful deconvolution. The presence of two peaks in the unit response function is a strong indication of the presence of multiple pathways during the tracer experiment.

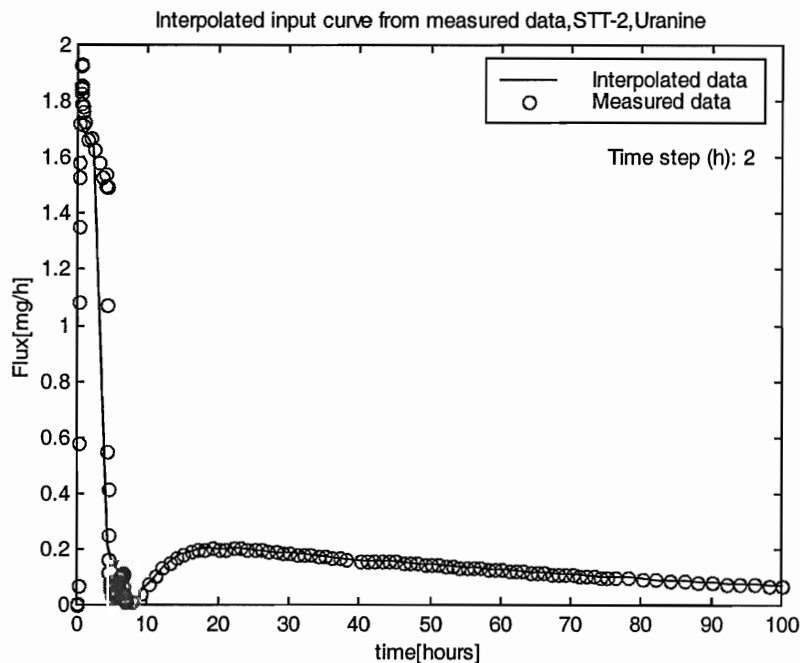


Figure 4-5 *Interpolated input curve for Uranine in STT-2.*

One step in the deconvolution procedure is the interpolation of injection data arrays to equal predefined time step. As an example of this step the interpolation of the Uranine injection curve is presented (Figure 4-5). This interpolation procedure was performed successfully on all the tracers.

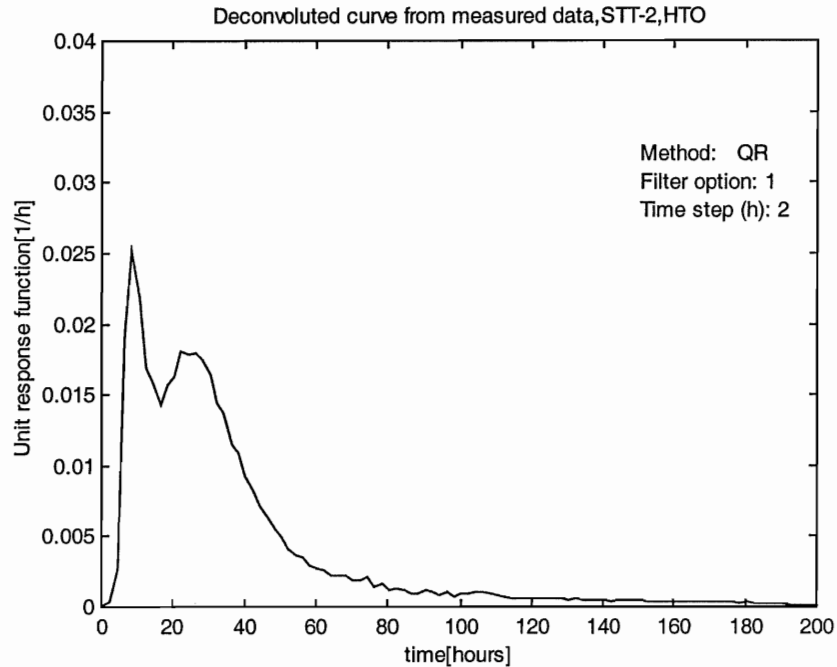


Figure 4-6 Unit response function for HTO in STT-2.

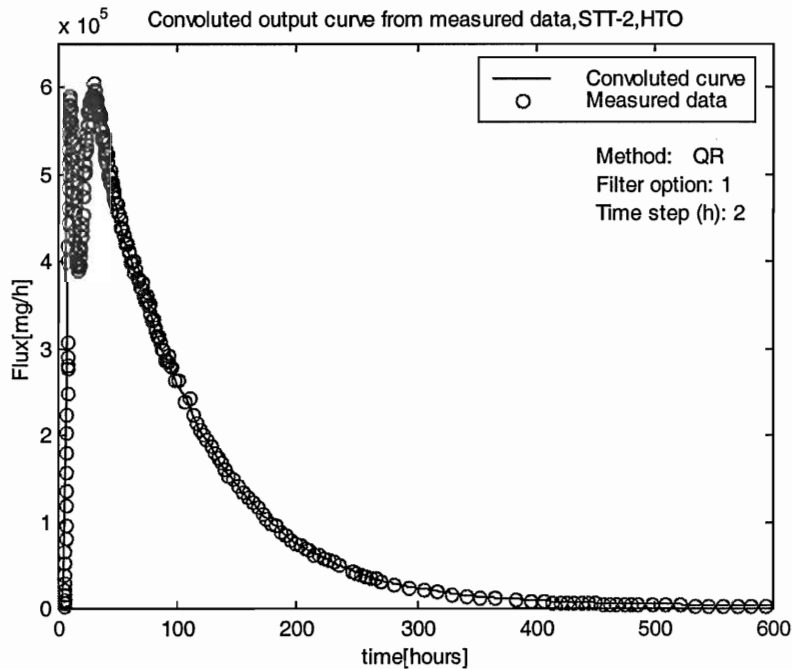


Figure 4-7 Convoluted unit response function for HTO in STT-2 compared with measured data.

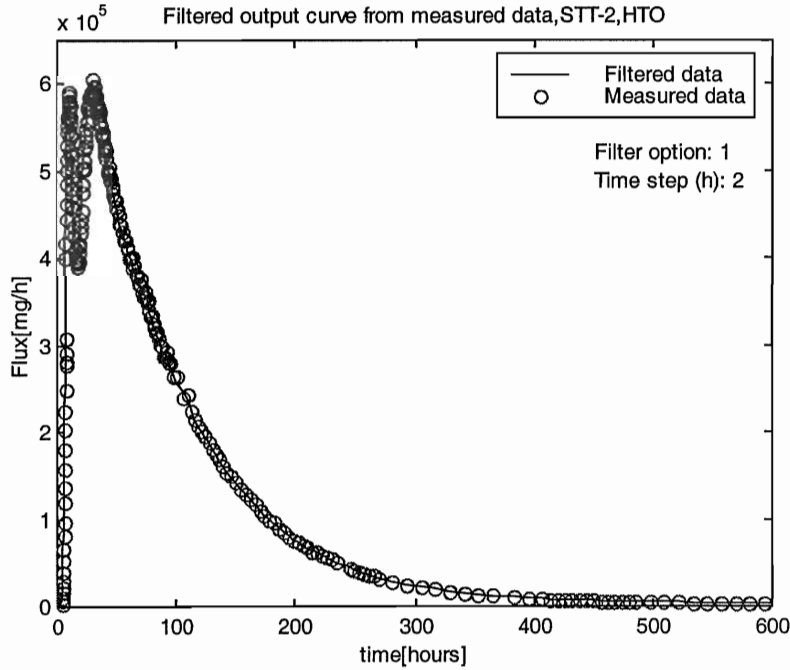


Figure 4-8 Original and filtered output data for HTO in STT-2.

The unit response function for HTO has a similar appearance to that of Uranine except for a slightly larger tailing. For HTO a 3-step filtering was necessary, as the experimental breakthrough curve was noisy.

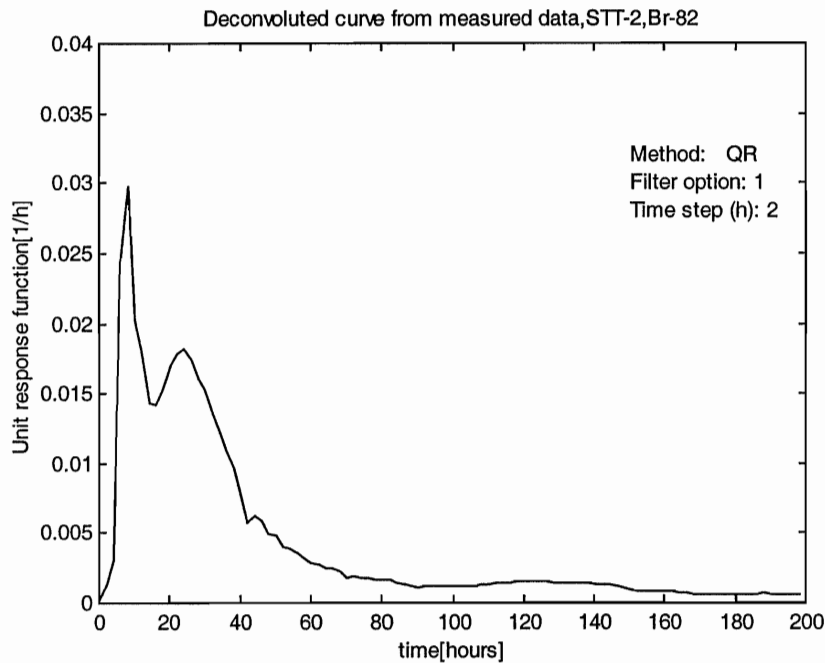


Figure 4-9 Unit response function for Br-82 in STT-2.

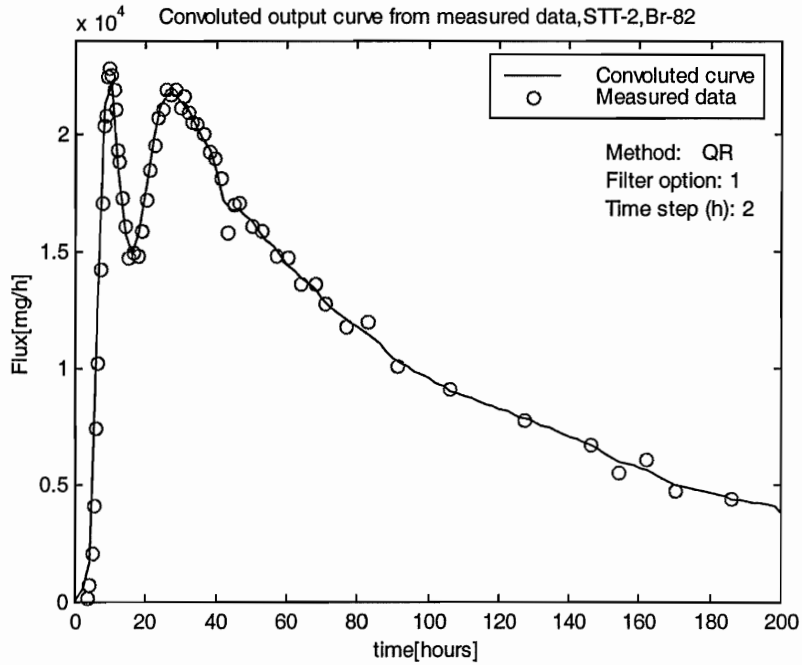


Figure 4-10 Convoluted unit response function for Br-82 in STT-2 compared with measured data.

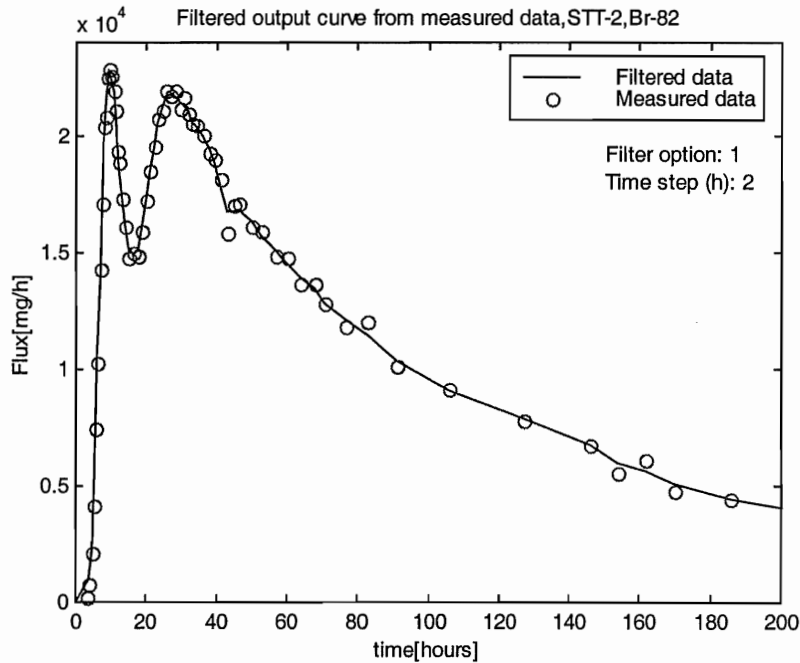


Figure 4-11 Original and filtered output data for Br-82 in STT-2.

The unit response function for Br-82 is consistent with those of Uranine and HTO, i.e. two distinct peaks. A 3-step filtering on the breakthrough curve was needed in order to achieve a smooth response function.

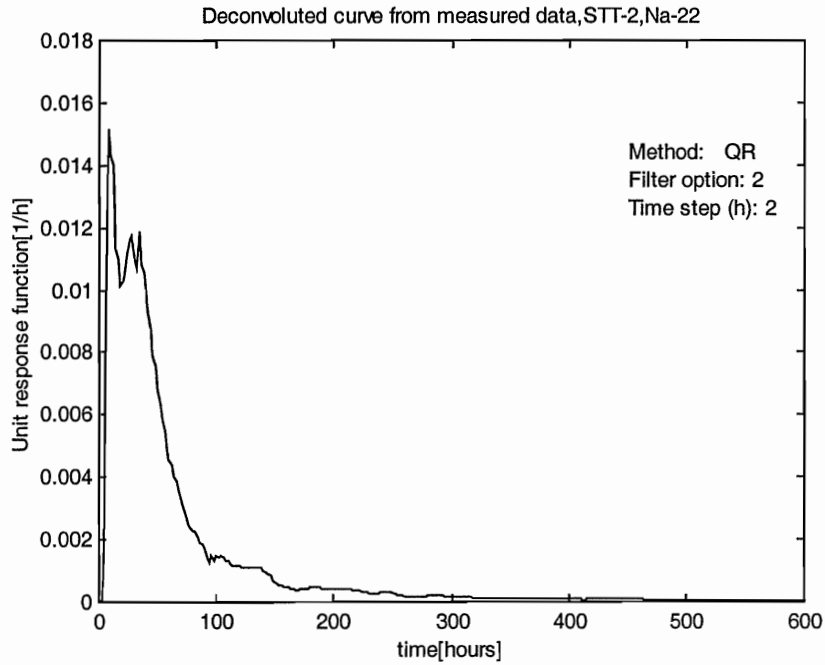


Figure 4-12 Unit response function for Na-22 in STT-2.

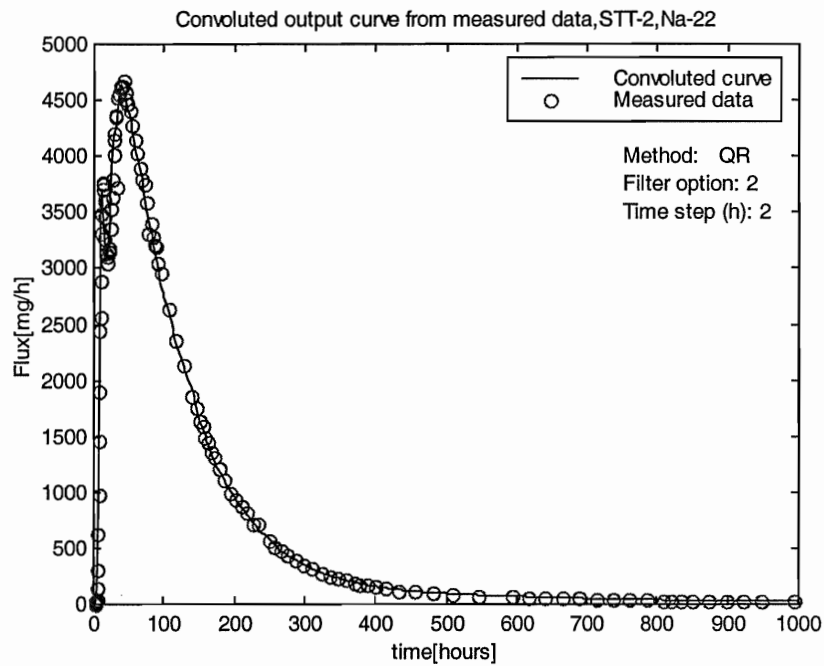


Figure 4-13 Convolved unit response function for Na-22 in STT-2 compared with measured data.

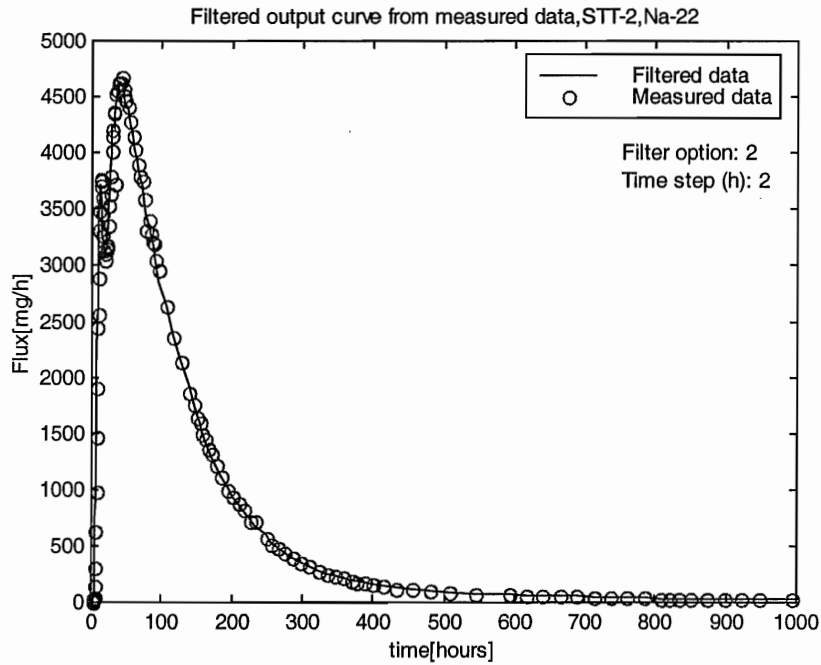


Figure 4-14 Original and filtered output data for Na-22 in STT-2.

The unit response function of Na-22 also shows two peaks like Uranine, HTO and Br-82, but the release is to some extent delayed in time with a more pronounced tailing. The second peak in the unit response function is less distinct than for Uranine, HTO and Na-22.

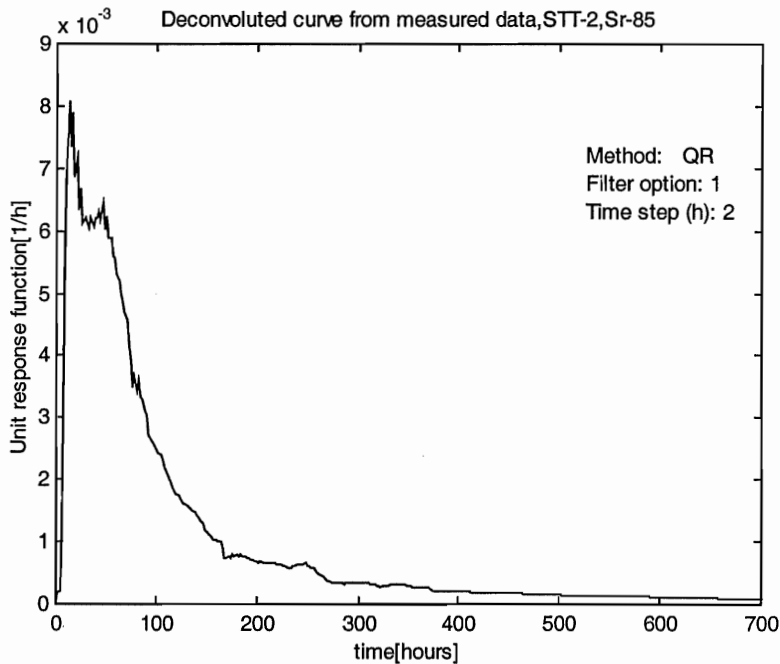


Figure 4-15 Unit response function for Sr-85 in STT-2.

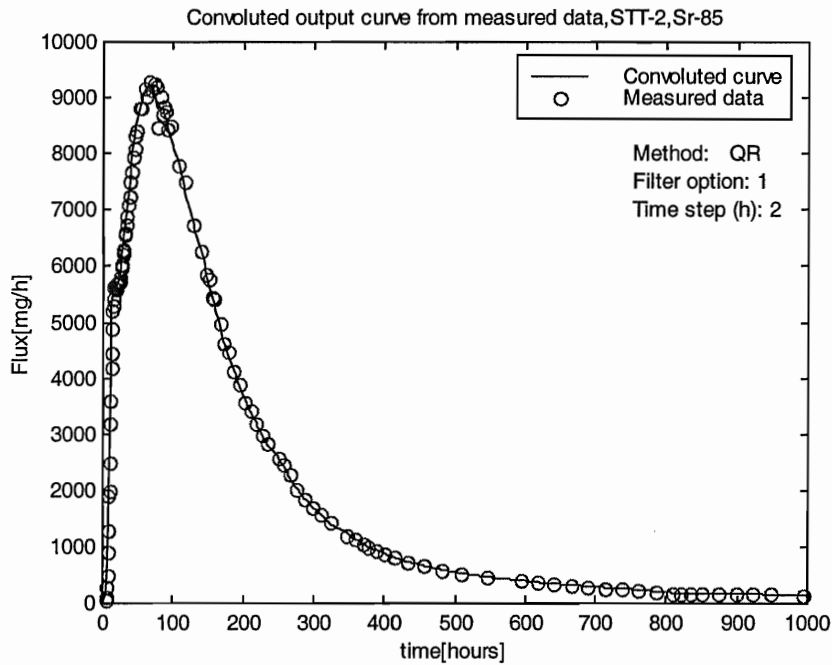


Figure 4-16 Convoluted unit response function for Sr-85 in STT-2 compared with measured data.

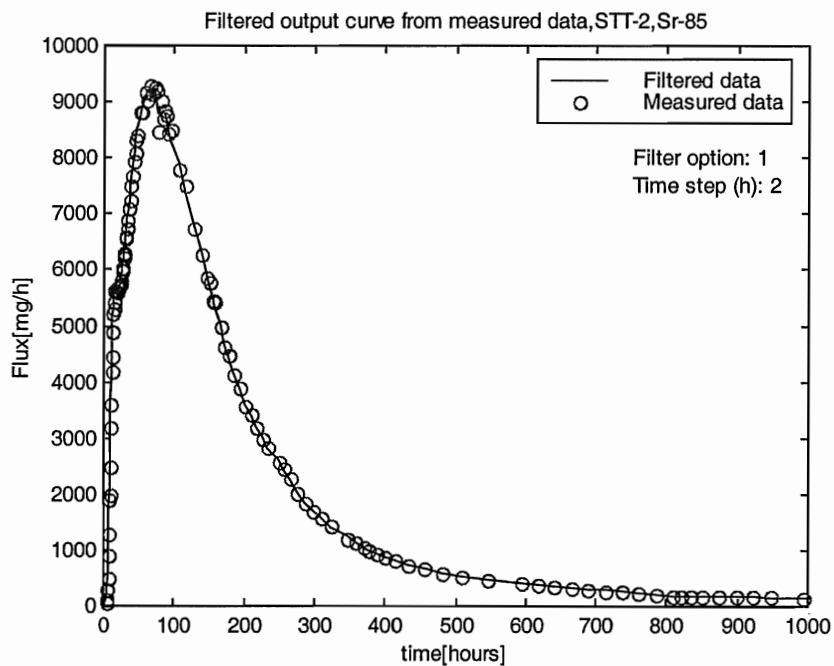


Figure 4-17 Original and filtered output data for Sr-85 in STT-2.

As for Na-22 the unit response function of Sr-85 is considerably lower than of Uranine and HTO. The curve consists of two peaks but the second peak is small relatively the first one. For Sr-85 the unit response function is also more delayed in time with a clear tailing.

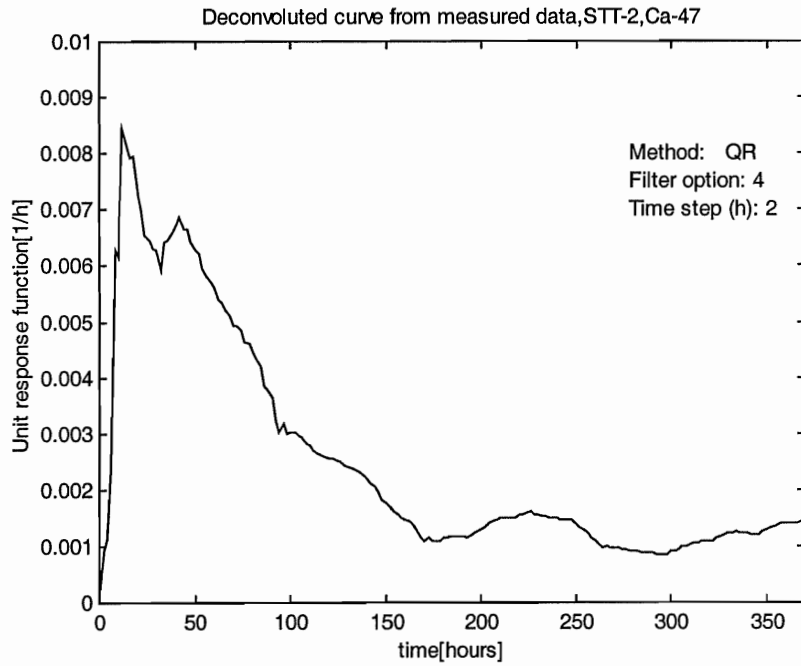


Figure 4-18 Unit response function for Ca-47 in STT-2.

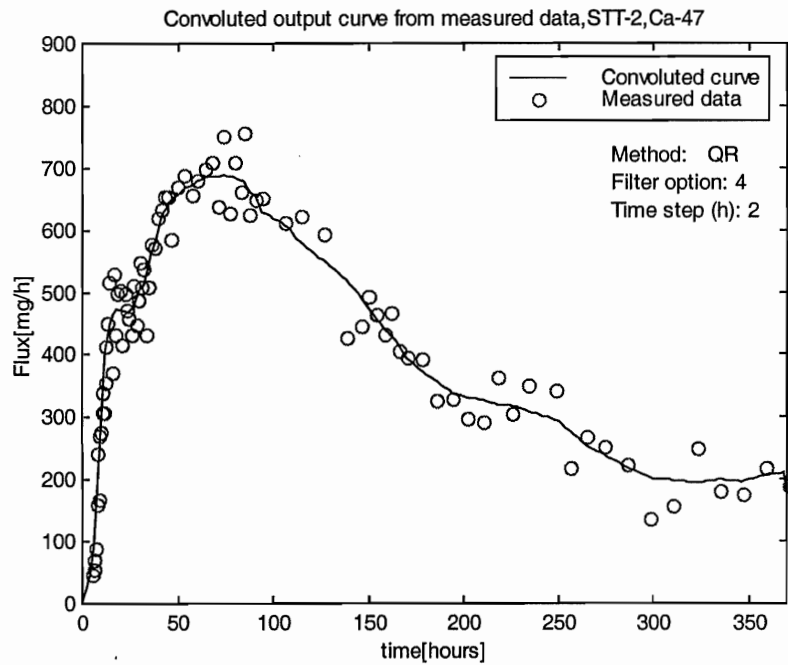


Figure 4-19 Convolved unit response function for Ca-47 in STT-2 compared with measured data.

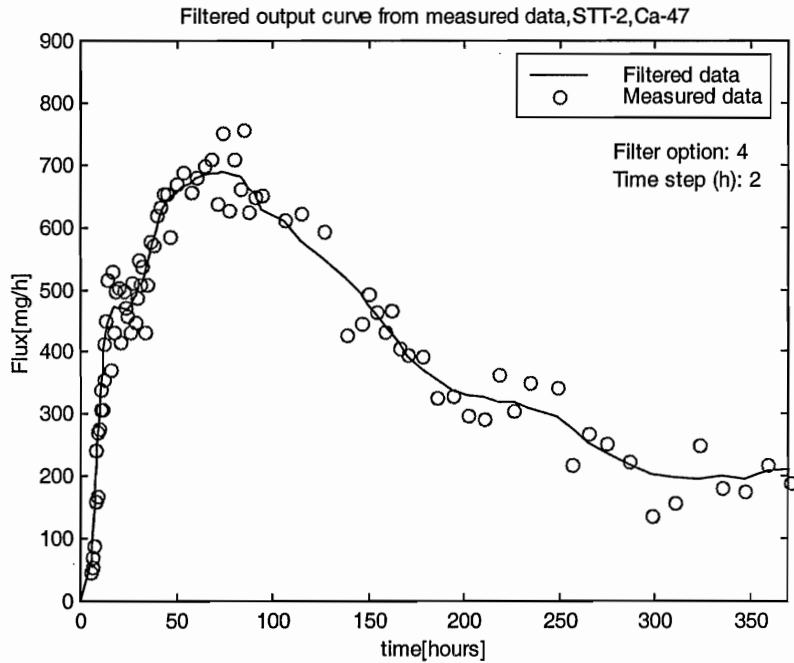


Figure 4-20 Original and filtered output data for Ca-47 in STT-2.

A high degree of filtering (9-step filter) of the breakthrough curve of Ca-47 was necessary before deconvolution as the curve was very irregular. The shape of the unit response function is relatively wide and two peaks are distinguishable. The shape of the unit response function after about 100 hours is most likely an artefact caused by the scattered data.

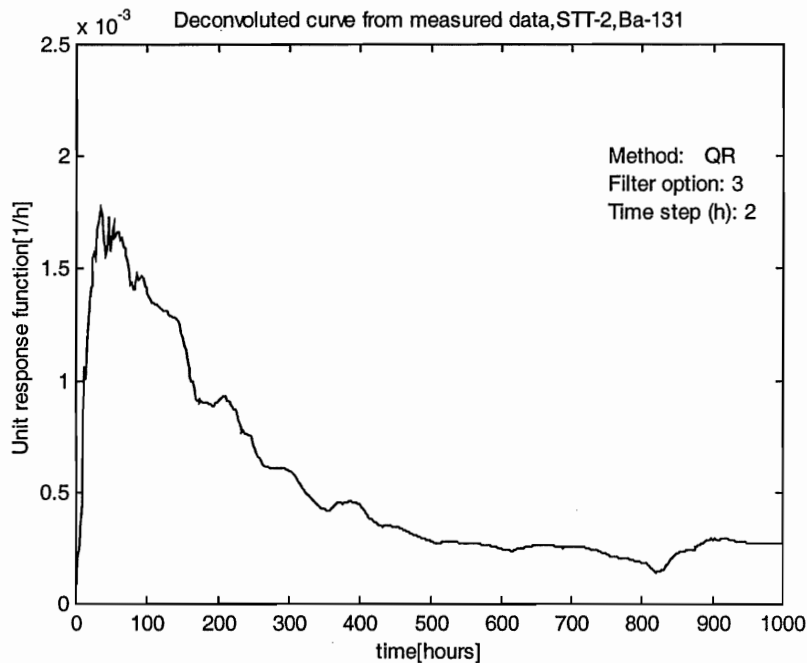


Figure 4-21 Unit response function for Ba-131 in STT-2.

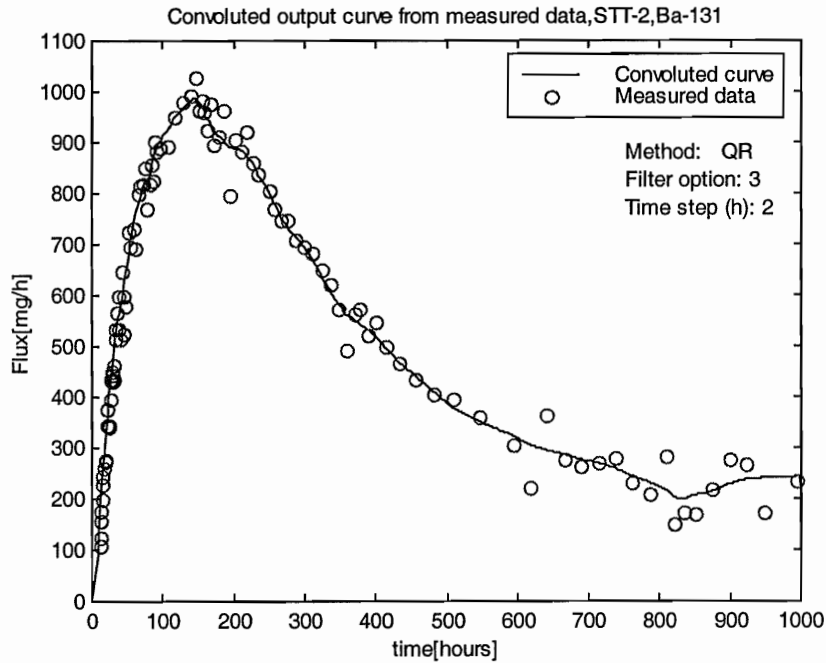


Figure 4-22 Convoluted unit response function for Ba-131 in STT-2 compared with measured data.

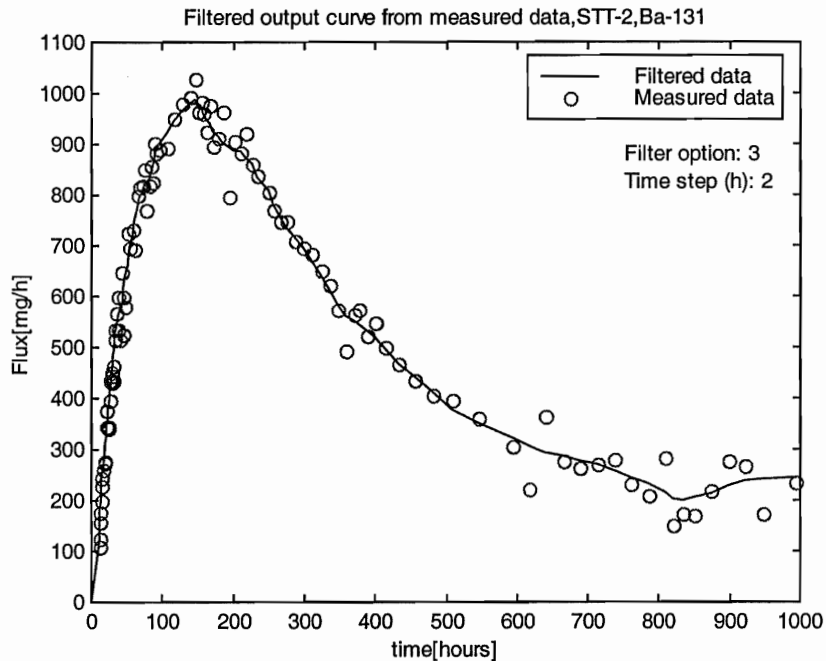


Figure 4-23 Original and filtered output data for Ba-131 in STT-2.

The breakthrough curve for Ba-131 was filtered (7-step filter) before deconvolution. The unit response function shows considerable tailing and consists of only one clearly defined peak. The irregular shape of the unit response function makes the possibility to identify a smaller second peak very small.

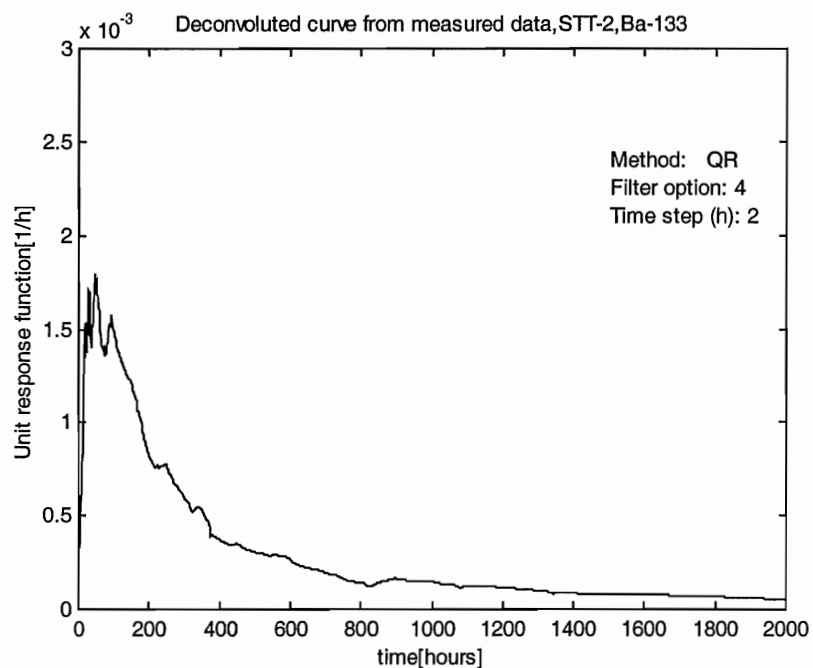


Figure 4-24 Unit response function for Ba-133 in STT-2.

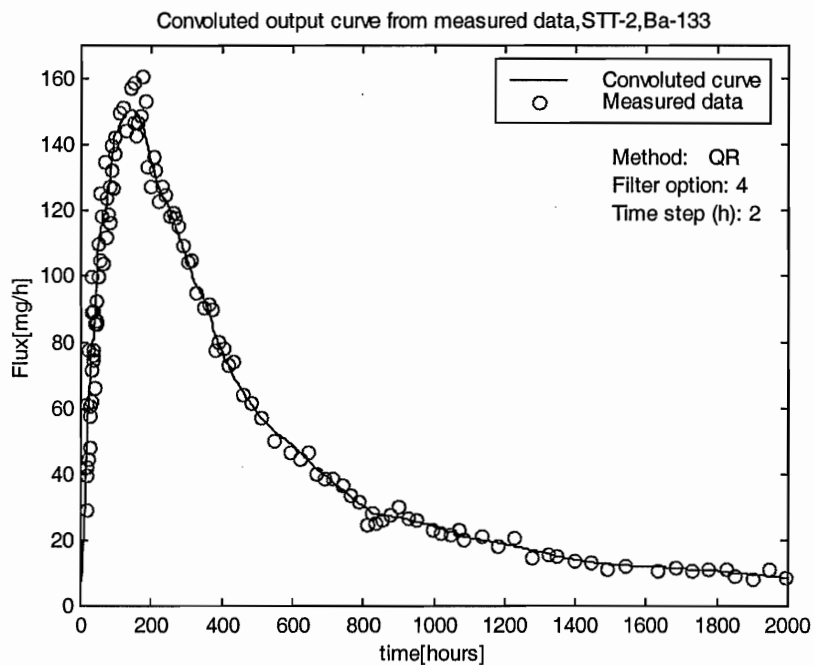


Figure 4-25 Convolved unit response function for Ba-133 in STT-2 compared with measured data.

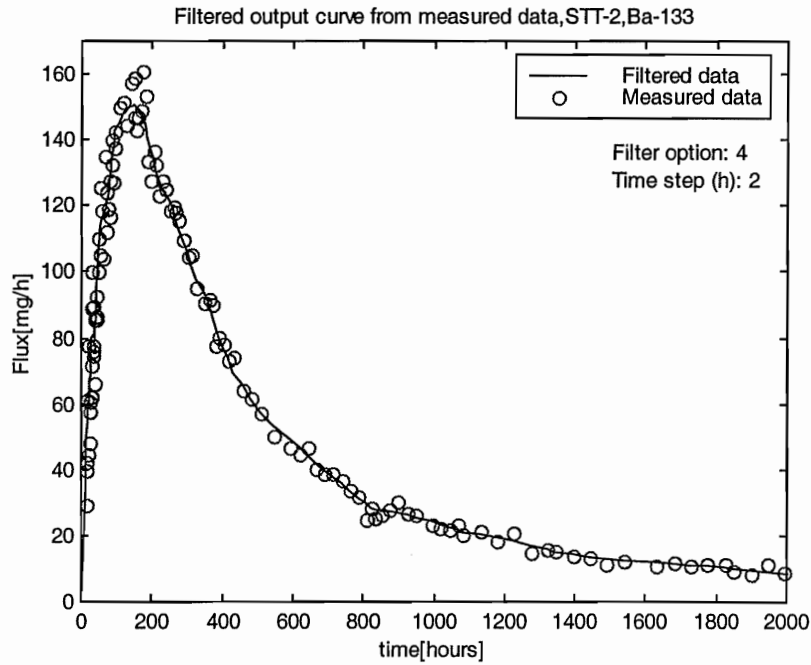


Figure 4-26 Original and filtered output data for Ba-133 in STT-2.

A higher degree of filtering was used for Ba-133 than for Ba-131 (9-step filter) than for The unit response function of Ba-133 are similar to those of Ba-131, with the exception that there are more oscillations in the peak.

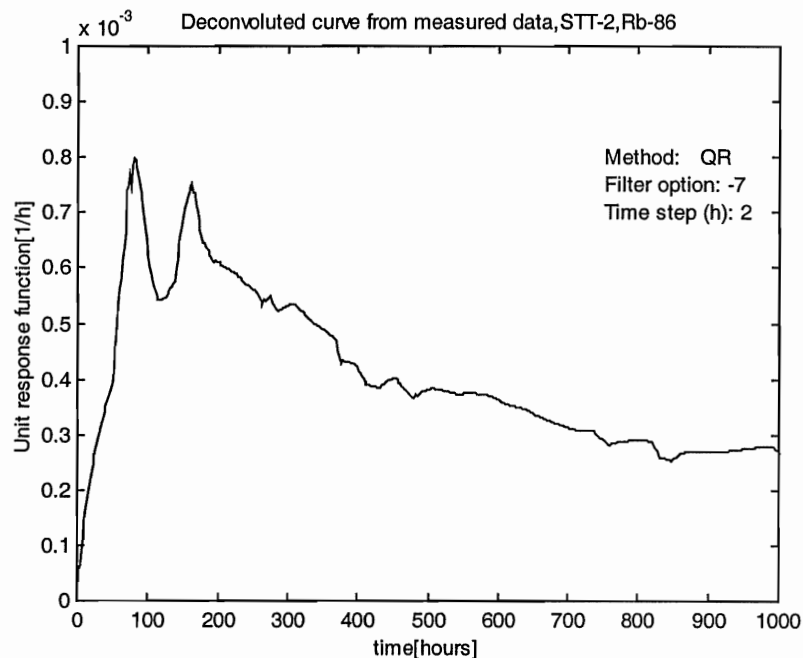


Figure 4-27 Unit response function for Rb-86 in STT-2.

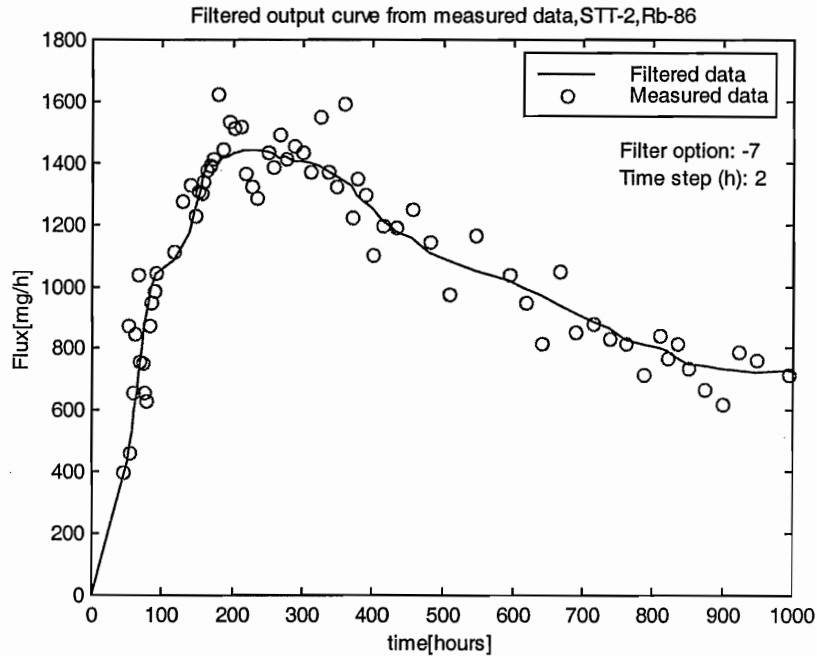


Figure 4-28 Original and filtered output data for Rb-86 in STT-2.

The Rb-86 breakthrough curve was very scattered resulting in a number of artificial peaks. The degree of filtering was varied, see Section 4.3. The number of peaks is significantly reduced when using an extensive filtering. However, two peaks remain also after filtering using a 15-step uniform filter. It is not clear whether these peaks are artefacts caused by the deconvolution or are caused by the presence of multiple pathways.

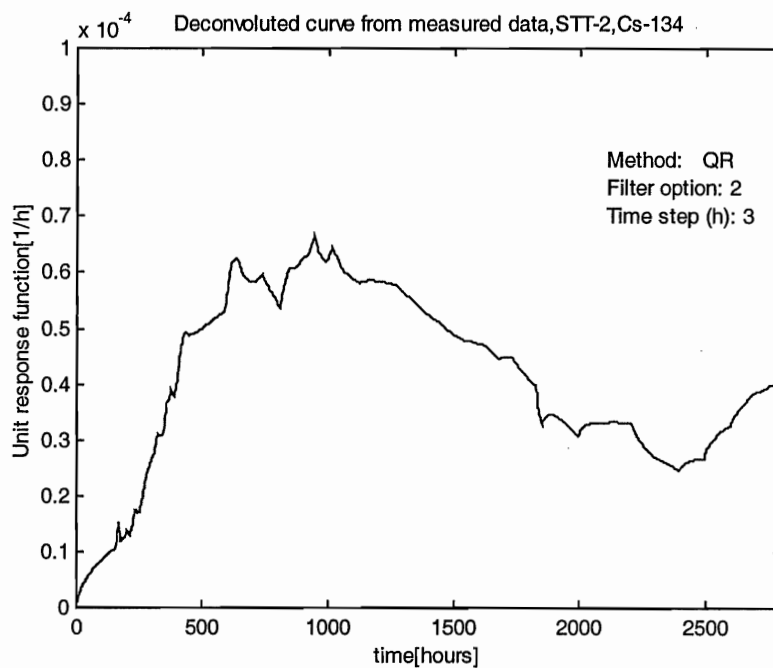


Figure 4-29 Unit response function for Cs-134 in STT-2.

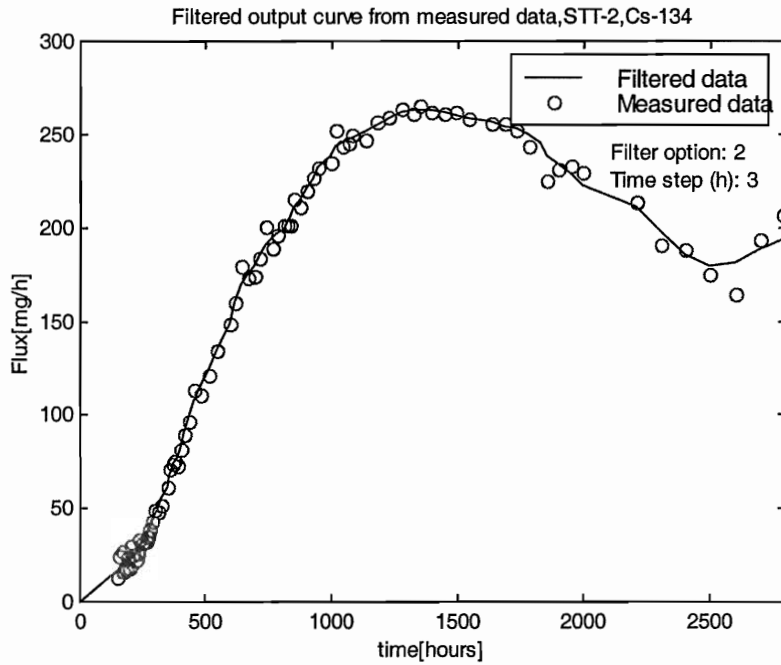


Figure 4-30 Original and filtered output data for Cs-134 in STT-2.

The unit response function of Cs-134 is somewhat irregular due to small oscillations in the breakthrough curve. A sharp increase in flux at the end of the breakthrough curve causes also gives rise to an increase in the breakthrough curve after 2500 hours. This is most likely an artefact of errors in the experimental data.

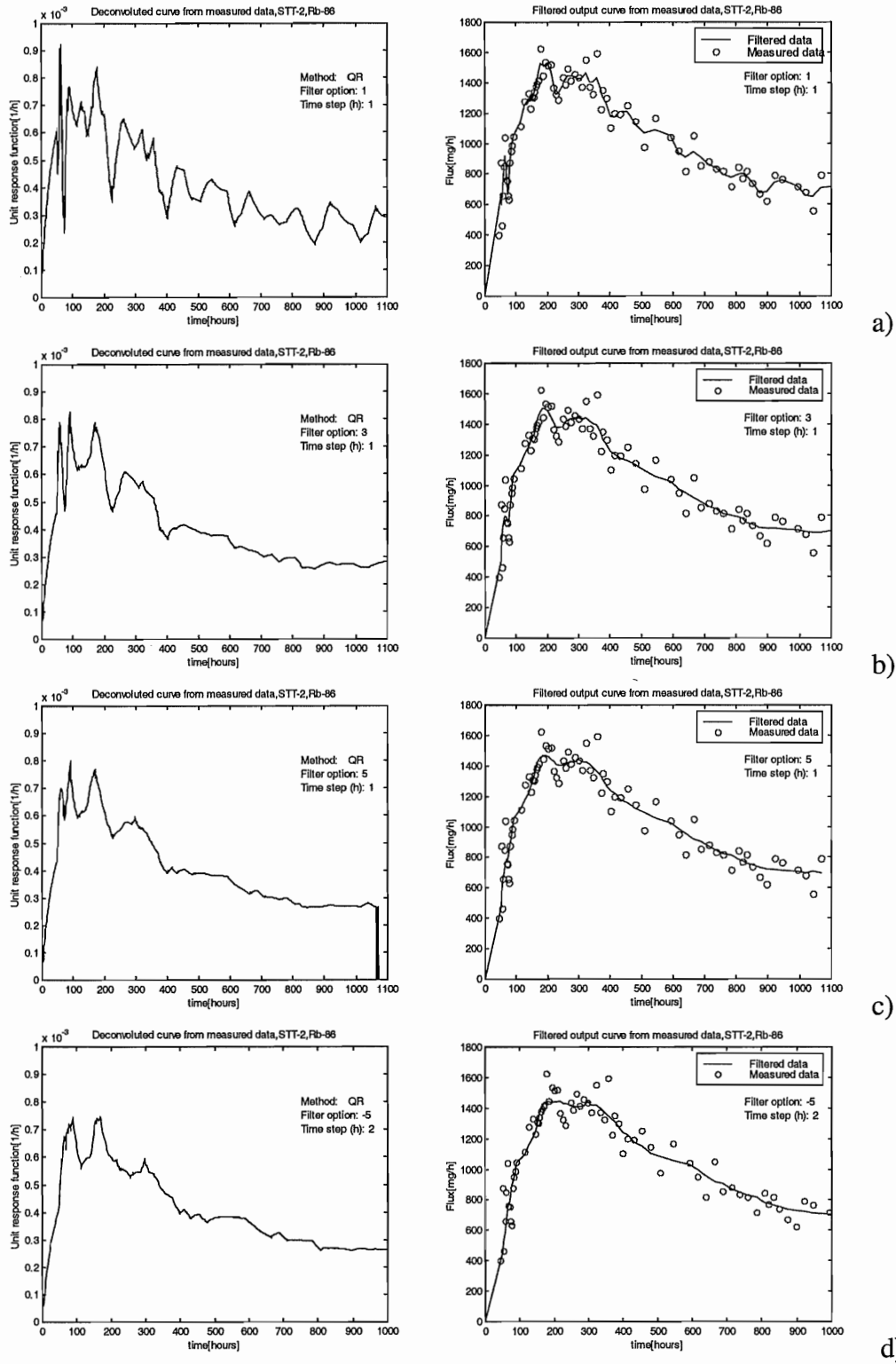


Figure 4-31 Effect of different filter length on the deconvolution of Rb-86 breakthrough in STT-2. Left hand column gives the unit response functions and the right hand column the filtered breakthrough curves. a) 3-step normal filter, b) 7-step normal filter, c) 11-step normal filter, d) 11-step uniform filter.

4.3 Variation of filter length

An evaluation was made of the importance of the length of the filter used for smoothing of the breakthrough curve. The test was performed for Cs-134 and Rb-86. Figure 4.31 a) – d) presents the results of the test for Rb-86. In the left hand column the unit response functions after deconvolution are presented and in the right hand column the filtered breakthrough curves. For Rb-86 the breakthrough curve was very noisy making deconvolution difficult.

In Figure 4.31 a) a 3-step normal filter was used which is insufficient to smoothen the breakthrough curve with prominent oscillations in the unit response function as a result. In b) a 7-step normal filter was used, which is sufficient to smoothen the end of the tail of the breakthrough curve. However, oscillations are still apparent at the peak of the breakthrough curve resulting in a spiky appearance of the deconvoluted curve. An 11-step normal filter leads to some improvement, but the main spikes remain. In Figure 4.31 d) an 11-step uniform filter was used, which results in slight reduced spikes in the unit response function. As a consequence of this a 15-step uniform filter was used in the evaluation, see Figures 4.28 and 4.28.

4.4 Test of extreme smoothing

An evaluation was also made of the effect of extreme smoothing of the breakthrough curve of Cs-134. In this case a polynomial fit was made for the breakthrough curve, see Figure 4.32. The resulting unit response function is presented in Figure 4.33. Since the breakthrough curve is completely smooth also the unit response function becomes smooth. The tail of the unit response function initially declines, but after about 2000 hours starts to level out.

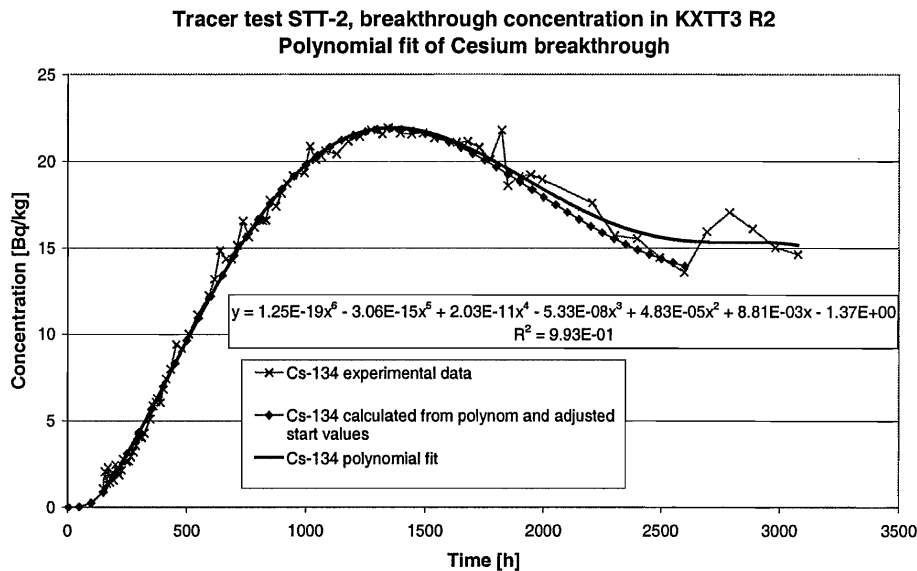


Figure 4-32 Original and fitted breakthrough data for Cs-134 in STT-2.

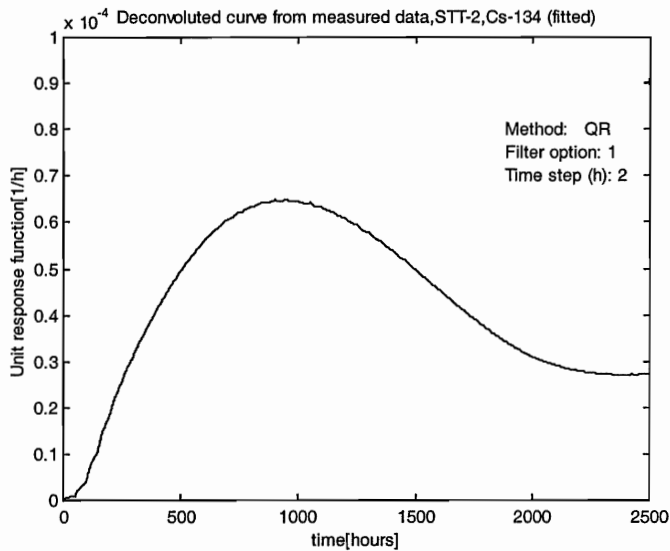


Figure 4-33 Unit response function for Cs-134 in STT-2, the output data in the deconvolution calculation is calculated from the function fitted on experimental breakthrough curve.

4.5 Compilation of results

In Figure 4-34 the unit response functions of all tracers from STT-2 have been compiled in one figure in order to facilitate the comparison between the different tracers. The double peak is apparent in the unit response functions of Uranine, HTO, Br-82 and Na-22. An indication of a double peak is also apparent for Sr-85 and Ca-47.

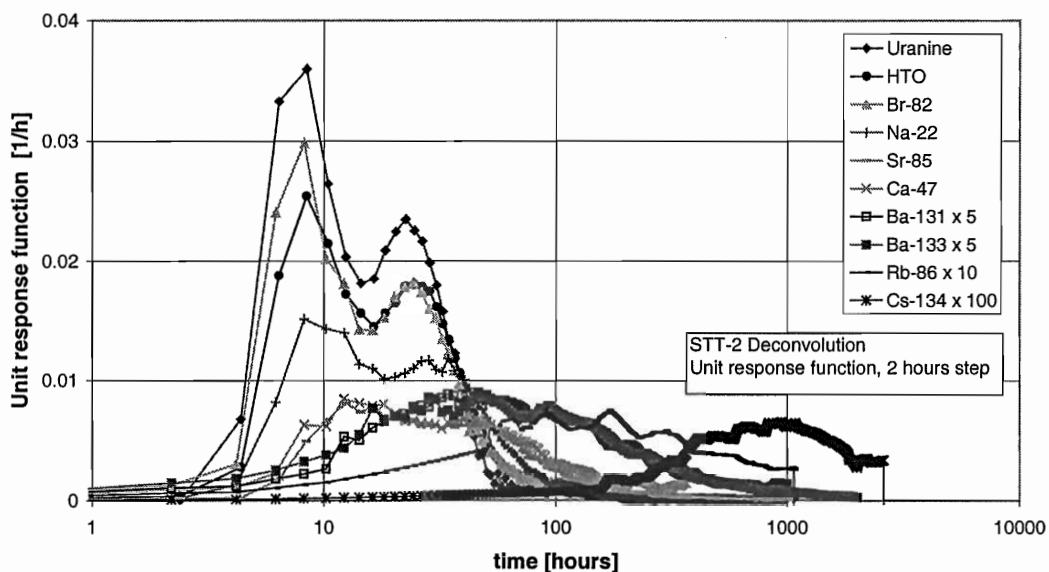


Figure 4-34 Unit response functions for tracers in STT-2.

5 Discussion and conclusions

5.1 Deconvolution approach

The use of deconvolution to obtain unit response functions for tracers can be very helpful in evaluating tracer experiments, since the unit response functions only contain features which are due to transport processes and not affected by the shape of the injection curve. Thus, the effects such as dispersion and mass transfer may be visualised even with long injections.

Unit response functions can be helpful in a comparison between model predictions and experimental curves. In comparisons of breakthrough curves for tests with long injection periods it may be difficult to distinguish the features that are introduced by the shape of the injection curve from those due to transport processes. Many of the mathematical models used within Task 4E and 4F derive unit response functions as a part of the transport calculations, or may give such functions as output if desired. A comparison between unit response functions predicted by models and those derived from the experimental data will give information on how well the models describe the actual transport processes.

The disadvantage is that the procedure involves a mathematical manipulation of the data, and since deconvolution is an ill-posed mathematical problem this may give rise to numerical problems. It may therefore be difficult to distinguish between physically relevant features from mathematical peculiarities. In the method used for the present study problems concerned getting a fine enough resolution to reveal the details for the non-sorbing or very weakly sorbing radionuclides and to get an acceptable deconvolution for radionuclides with very noisy breakthrough curves.

5.2 Deconvolution methods

The deconvolution method used in this study is relatively simple. More sophisticated methods have been developed, for example the Extreme Value Estimation (EVE). However, the majority of the experimental curves were of very good quality, with only few or no outlying values. Thus, successful deconvolution could be for all of the tracers used in STT-2. The unit response functions obtained included more detail than the curves obtained from the STT-1 and STT-1b tests. This is partly due to the lower flow rate used in the STT-2 test giving longer travel times and partly due to the improvement of the deconvolution techniques, particularly the techniques used for filtering of the breakthrough curves. Also the computer code used for the deconvolution has been improved allowing for a more efficient use.

The present method may be developed to improve the obtained unit response functions and to ensure a successful deconvolution also of the remaining tracer tests:

- In the case of non-sorbing radionuclides a much shorter time step than proved to be numerically stable would be needed to determine the detailed characteristics of the peaks. Improvement of the stability of the method or the use of more stable methods is therefore desirable.
- The method of filtering spiky output data needs to be developed.

5.3 Conclusions

Deconvolution of experimental breakthrough curves using the injection curve in order to obtain a unit response function is a useful approach to evaluate tracer experiments in order to identify features in the breakthrough curves caused by transport processes and not caused by the shape of the injection curve. In particular they can be used for comparison with unit response functions obtained from model predictions.

For the STT-2 test the double peak present in the breakthrough curve remains in the unit response function after deconvolution. This is an indication that the double peak is not an effect of the injection procedure, but an effect due to the presence of multiple pathways during the tracer test.

The method presently used for deconvolution has successfully deconvoluted all of the tracers used in the STT-2 test. However, there is a need for further improvement of the method in order to obtain a better resolution for non-sorbing tracers and to handle curves with oscillations due to large experimental errors.

References

Andersson P, Johansson H, Nordqvist R, Skarnemark G, Skålberg M, Wass E, 1998. TRUE 1st stage tracer test programme, Tracer tests with sorbing tracers, STT-1, Experimental description and preliminary evaluation. Äspö Hard Rock Laboratory Technical Note TN-98-10t, Swedish Nuclear Fuel and Waste Management Co.

Andersson P, Johansson H, Skarnemark G, Skålberg M, Wass E, 1999. TRUE 1st stage tracer test programme, Tracer tests with sorbing tracers, STT-1, Experimental description and preliminary evaluation. Swedish Nuclear Fuel and Waste Management Co.

Elert M, Svensson H, 1999. Deconvolution of breakthrough curves from TRUE-1 tracer tests (STT-1 and STT-1b) with sorbing tracers. Äspö Task Force Task 4F, International Progress Report, IPR-99-35, Swedish Nuclear Fuel and Waste Management Co.,

Ilvonen M, Hautojärvi A, Paatero P, 1994. Intraval project phase 2, Analysis of stripa 3D data by a deconvolution technique. Nuclear Waste Commission of Finnish Power Companies, YJT-94-14.

Skaggs T H., Kabala Z J, Jury W A, 1998. Deconvolution of a nonparametric transfer function for solute transport in soils, *Journal of Hydrology*, 207, 170-178.

Tsang C F, Tsang Y W, Hale F V, 1991. Tracer transport in fractures: Analysis of field data based on a variable-aperture channel model, *Water Resources Research*, 27, 3095-3106.